Research and Innovation action
NUMBER — 955387 — LEON-T

LEON-T

Low particle Emissions and lOw Noise Tires

Deliverable No.	2.3 Chemical transformation and health hazard evaluation	
Deliverable Title	Results from chemical transformations of tire organic compounds and volatiles and health hazard potential classification	
Dissemination	PU	
Written by	Peter Tromp, Henrik Cornelisson van de Ven, Alex van Renesse van Duivenbode, Mark Dicks, Henk de Weerd, Jos van Triel	
Checked by	Joris Quick & Marcel Mathissen	29-04-2024
Approved by	Juan J García (IDIADA)	29-04-2024
Issue date	01-05-2024	

This Project has received funding from the European Union´s Horizon 2020 research and innovation programme under grant agreement N° 955397.
The content of this report reflects only the author´s view CINEA is not reponsible for any use that may be made of the information it contains.

Revision History

REVISION	DATE	DESCRIPTION	AUTHOR (ORGANIZATION)

Contents

Abbreviations and Units

ALI	Air Liquid Interface
BR	Polybutadiene
EC	Elemental carbon
GC	Gas Chromatography
MS(MS)	(tandem) mass spectrometry
ISO	International Organization for Standardization
LC	Liquid Chromatography
Leon-T	Low particle Emissions and lOw Noise Tires
MP	Microplastics
NR	Natural rubber
OC	Organic carbon
OP	Oxidative Potential
PM	Particulate matter
PM10	Particulate matter with an upper limit of 10 µm
PM2.5	Particulate matter with an upper limit of 2.5 µm
PM1	Particulate matter with an upper limit of 1 µm
PSD	Particle size distribution
SBR	Styrene-butadiene rubber
TED	Thermal Extraction and Desorption
TGA	Thermogravimetric analysis
TSP	Total Suspended Particles
TRWP	Tire and road wear particles
TWP	Tire wear particles

1 Introduction

1.1 Background

Since the early 1990s much research has focussed on the link between airborne particulate matter (PM) and negative health effects [1], [2]. Air pollution, including PM, has been shown to lead to increased mortality with a specific link between PM and mortality through cardiopulmonary and respiratory diseases [3], [4]. Many attempts have been made to identify PM sources, particularly in urban settings where air quality is worse and population density is higher [5], [6]. Source apportionment studies using methods such as Positive Matrix Factorisation (PMF) and Principal Component Analysis (PCA) have been carried out in cities around the world and suggest that traffic/automotive emissions contribute 10-15% to urban PM10 concentrations [7], [8]. Automotive emissions can be further separated into exhaust emissions (EE; soot, oil etc.) and non-exhaust emissions (NEE; tire, brake and road wear), where it is estimated that NEE contributes >5% total PM10 emissions [9]. A more recent 2023 source apportionment study which separated exhaust and non-exhaust emissions have given much higher numbers, assigning 28% PM10 to traffic with the majority of this (~87%) being NEE, highlighting the dynamic nature of the PM challenge [10]. While legislation has focused on reducing EE since the introduction of Euro 1 standards in 1992 (albeit at 0.14 g/km and only for diesel engines) [11], NEE have only been named for the first time in Euro 7 standards expected to come into force in 2025 [12].

An important source of NEE are tire and road wear particles (TRWPs), which contribute about 10% to the total airborne non-exhaust particles [13]. Formed due to the abrasion of the tire during driving, these particles are complex mixtures of tire rubber with mineral encrustations released from the road surface [14]. Per capita emission of TRWPs has been estimated to be 0.81 kg/year, of which 12% (0.1 kg/year) has been estimated to be released to the air [13]. Experimental measurement campaigns (excluding source apportionment studies) have been carried out in America, Europe and Asia and have reported TRWP PM10 concentrations of 0.05-2.2 $\mu g/m^3$ [15]–[17] and PM2.5 concentrations of 0.004-0.15 $\mu g/m^3$ [15]. This results in estimated TRWPs contributions of <1% and 0.1-10% to PM2.5 and PM10, respectively [16][18]. These particles formed during the interaction of tires and roads are mostly micro-sized conglomerates of tire and road material, but can also be formed as nano-sized particles from evaporative emissions due to heating of the tire followed by condensation and coagulation [19]. For predicting negative health effects and environmental impact of TRWP accurate information on tire wear generation, particle sizes and organic constituents including chemical transformations is essential. Besides, the generation of submicron and ultrafine particles, which seems to originate from organic constituents due to heating of the tires, is not well understood.

The health effects of TRWPs extend further than solely particle effects. Although some studies performed also chemical characterisation [20] of these particles, there is still limited information regarding organic constituents [21] and the chemical composition of airborne TRWP. Tire rubber is a complex mixture with up to 50 wt% additives, including particle additives, antioxidants/ozonants, vulcanisation agents and catalysts, and softening oils [22]. Common additives include Zn, sulphur, benzothiazoles and polyaromatic hydrocarbons (PAHs) [23]. These additives have the ability to leach out of TRWPs in the body or environment and are therefore also termed leachate. The leachability, environmental degradation and toxicological effects of these additives have been the focus of numerous studies [24]–[27]. The leachate we are exposed to via inhalation of airborne particles is not necessarily the same as the pristine formulation of the tire rubber. TRWP-PM_{10} can stay airborne for a number of weeks, during which time they may be exposed to both abiotic and biotic environmental stressors. These environmental stressors may result in the chemical transformation of some additives, thereby changing the toxicological risk of the additive [28]. For example, 6-PPD is a commonly used antiozonant, however the ozonation product formed during the rubber's lifetime, 6-PPDQ, has been shown to be lethal to certain species of salmon [29]. In contrast, it has also been shown that particles from pristine tires can be more toxic than those of worn tires. The authors attributed this to the higher levels of 1-octanethiol and certain PAHs in pristine than aged TRWPs [30].

A number of studies have investigated the influence of UV-ageing on the chemical transformation of leachates. Unice *et al.* used liquid chromatography with tandem mass spectrometry (LC-MSMS) to investigate the environmental availability of two vulcanisation agents (CBS and DPG), an antiozonant (6-PPD) and 13 of their transformation products throughout the product lifetime [31]. They found that each stage of the life cycle – curing, wearing, weathering – contributed to differences in transformation and availability. During weathering they suggest that initially low boiling point species are removed from the surface while after longer periods the targeted components were lost due to oxidation. Thomas *et al.* investigated the influence of freeze-thaw, wet-dry and UV-accelerated ageing on the transformation of additives. Using GC-MS non-target screening they found numerous benzothiazole derivatives as thermal transformation products and ketones, epoxides and carboxylic acids as photo-oxidation (UV) transformation products [32]. Interestingly, the much reported 6-PPDQ transformation product of 6-PPD was not identified, however the authors do note this may be due to the sensitivity of the analytical technique used. Until now, work on additives, leaching and chemical transformation has been limited to soil and aqueous environments. This leaves a large knowledge gap regarding these chemical transformations with relevance to air pollution [33]. Also for aerosol particles in the atmosphere transformation processes induced by photochemically aging influence the physicochemical properties and therefor health hazard. For the investigation of atmospheric transformation (oxidation) processes and secondary aerosol formation environmental aging chambers and oxidation flow reactors are commonly used. For the latter, accelerated aging with high intensity UV radiation and high concentrations of oxidative species is involved and it remains questionable how representative the chemistry within these flow reactors are for atmospheric transformation processes [36].

1.2 Objective and study approach

In the LEON-T project, we aim to identify, measure, characterise and compare, through both in-lab and on-road experiments, the particle emissions from vehicle tires under different driving conditions. The current report focusses on the physicochemical characterisation of emitted particles and volatiles, the identification of the potential chemical transformation processes and most importantly the evaluation of their associated health hazard.

For this objective, TNO, RIVM and VTI have performed an in-lab test campaign at VTI's road simulator facilities, with real-time particle monitors, gas and size-selective particle sampling techniques and the VACES-BioSampler where particles are sampled in liquid suspensions which allows for direct in-vitro toxicity testing. The sampled particles were subjected to an accelerated UV-ageing program to simulate the short-term (~2 weeks) UV exposure of particles. Both freshly generated particles and UV-aged TRWP as well as emitted volatiles were analysed using several target and non-target techniques, which includes i.e. (double-shot) TGA-TED-GCMSMS. Tires from different market segments (budget/executive, summer/winter/4season) were individually sampled to investigate the influence of different tire characteristics, formulations and additives.

Moreover, toxicological analysis of the freshly generated particles were performed via in-vitro studies by means of a 'quasi-ALI' exposure system where A549 human alveolar epithelial cells were exposed to different concentrations of PM suspensions. Toxic effects, including cytotoxicity, viability, metabolic activity and release of pro-inflammatory cytokines were studied. In addition, a newly developed oxidative potential assay was performed on freshly generated and transformed species. Physicochemical and toxicological data were combined to explore the possibilities for an integrated hazard potential for tire emissions. Insights into the short-term chemical transformations that occur for airborne particles will further improve accurate risk assessments and inform potential legislation surrounding their use.

2 Methodology

The study approach consists of several steps:

1. Selection of representative car tires (Section 2.1) and a chemical characterisation of these tires (Section 3),
2. In-lab tests with selected tires with a circular road simulator at VTI's road simulator facilities (Section 2.2) and collection of emitted particles and volatiles (Section 2.3),
3. Off-line accelerated UV aging of emitted particles in an aging chamber (Section 2.4),
4. Chemical characterisation of volatiles and freshly generated and UV aged particles (Section 3),
5. Toxicological analysis of freshly generated particles (fine and coarse fraction) via in-vitro studies by means of a 'quasi-ALI' exposure system and UV aged particles via analysis of oxidative potential (Section 4).

2.1 Selection of tires

The tire selection includes 3 different summer tires as well as an all season and a winter tire. Different season tires are coming from the same manufacturer (Continental). For summer tires, tires from three different brands are tested: Continental, Goodyear and Ling Long (Table 1). In addition, a custom-made tire has been manufactured by LingLong with appr. 2% cobalt-boroacylate. This custom-made tire will be used in the on-road experiments, where cobalt will act as a tracer for tire wear abrasion (Deliverable 2.2). During the road simulation tests the particle emission characteristics of this custom-made tire will be compared with the other tires.

Table 1. Selected tires for the road simulator tests at VTI's road simulator facilities

Brand	Pattern Name	Season	Dimensions	Load/ Speed Index	Rolling Resistance	Wet Grip	Rubber hardness	Noise
Goodyear	Efficient Grip Cargo	Summer	215/65 R16C	109/107 T	B	C	69.5	B (71dB)
Continental	Eco Contact 6	Summer	215/65 R16	102H XL	A	A	67.2	B (71dB)
Continental	Winter Contact TS870	Winter	215/65 R16	102 H	C	B	58.2	B (71dB)
Continental	Van Contact 4Season	All Season	215/65 R16C	109/107 T	B	A	67.5	B (73dB)
LingLong	Green Max Van HP	Summer	215/65 R16C	109/107 R	C	B	64.4	B (72dB)
LingLong	Custom made with cobalt additive	Summer	215/65 R16C	109/107 R	-	-	67.0	-

2.2 Road simulator measurement campaign

The VTI circular road simulator is a unique carousel-like equipment, used to test wear and particle emissions of different combinations of pavements and tires (Figure 1). Particle sampling in the simulator hall makes it possible to sample wear particles with very low contamination from surrounding sources and no influence from tail-pipe emissions. The road simulator consists of four wheels that run along a circular track with a diameter of 5.3 m. A separate DC motor is driving each wheel and the speed can be varied up to 70 km h^{-1}. At 50 km h^{-1} an eccentric movement of the vertical centre axis is started to slowly undulate the tires over the pavement track. Any type of pavement can be applied to the simulator track and any type of personal car tire can be mounted on the axles. For the currents tests a concrete cement pavement is used. Concrete cement is a composite material consisting of a cementitious binder and aggregates. The cementitious binder is made of Portland cement paste. The aggregates are composed of crushed stones.

The simulation tests were performed from 5 October till 3 November 2022. The test runs were operated at 70 km h-1 during a consecutive period of 7 – 8 hours. Before and after the tests the tires were weighed. During the test time the simulator hall was closed and not actively ventilated, although the sampling equipment caused some ventilation and also pressure gradients might have caused minor self-ventilation. The volume of the simulator hall was appr. 802.5 m^3 and the ventilation caused by the sampling equipment (Section 2.3) was 85.5 m^3 h^{-1}. An internal air-cooling system was used to temperate the simulator hall at 20 °C. After each test the ventilation was switched on to clean the air in the simulator hall.

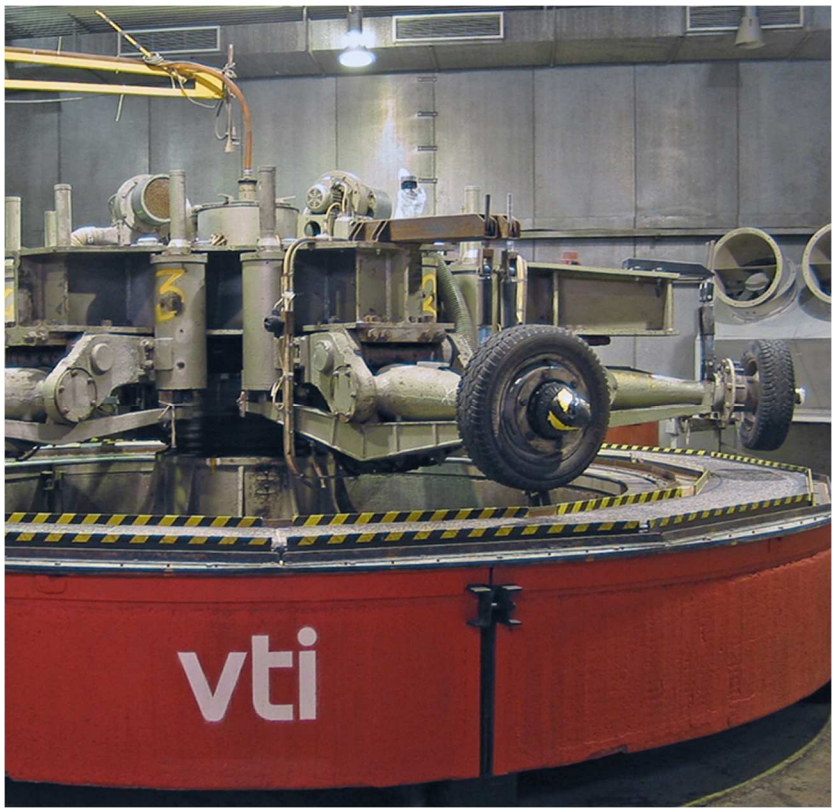

Figure 1. The VTI circular road simulator

2.3 Air sampling

During the circular road simulator tests air measurements were performed in the simulator hall. Measurements consist of real-time particle monitoring (see Deliverable 2.2) and particle collection and gas sampling for off-line physicochemical analysis and toxicity testing (Table).

Table 2. Sampling strategy during the road simulator testing

Particle collection	Gas sampling
- Filter sampling: TSP, PM_{10}, $PM_{2.5}$, PM_1 (Teflon + QMA), SEM (Nucleopore) - Cascade impactor: DLPI (30 nm – 10 µm) and DGI (0.2 – 2.5 µm) - VACES Biosampler (2.5 – 10 & <2.5 µm)	- Tenax adsorption tubes - XAD-2 adsorption tubes

2.3.1 Particle and gas sampling for physicochemical characterisation

For collection of PM size selective filter based techniques and multi-stage cascade impactors were used. The collected fractions were TSP (Total Suspended Particles), PM10, PM2.5 and PM1. The TSP fraction was collected using four open-face sampling heads; two of the TSP samplers were connected with an XAD-2 adsorption tube (XAD-2 400/200mg, 8 x 110mm, SKC) for the collection of volatiles. The PM10 fraction was collected using a PM10 sampling head (Anderson type 246B), while PM2.5 and PM1 were sampled with the same sampling head with a VSCC (very sharp cut cyclone) for further particle fractionation. With the use of a splitter the PM size fractions were simultaneously collected on 47 mm quartz (Whatman® QM-A quartz filters) and Teflon (Pall PTFE Membrane Disc Filters) filters, each at a flowrate of 8.35 L/min. The flowrate was kept constant by using a critical flow capillary. For analysis with SEM/EDX, PM was collected with 25mm open-face samplers on gold-coated polycarbonate filters (0.4 µm, 25 mm, Nuclepore), with a flowrate of 1 and 3 L/min. In addition to XAD-2 also two Tenax TA adsorption tubes (Tenax TA, 300mg, 6.4 x 89 mm, stainless steel, InterScience) were used for the collection of volatile components; the flowrate was set at 50 mL/min. All samplers were mounted on an aluminium frame. An overview of the offline collection of particles and volatiles is given in Figure .

Figure 2. The sampling set-up for collection of particles and volatiles

Additional size fractions were collected using two different multi-stage cascade impactors. These impactors use the principle of inertia to capture particles of a certain size class on collection plates. This results in a size classification based on their aerodynamic diameter. The Dekati Gravimetric Impactor (DGI) is a high sample flow rate cascade impactor with 4 stages, which was operated at 70 L/min, and allows for the collection of 3 size fractions: 0.2-0.5, 0.5-1 and 1-2.5 µm on 47mm quartz and teflon filters, with a 70 mm glass fibre (Pallflex Emfab) backup filter for the size fraction <0.2 µm. The Dekati Low Pressure Impactor (DLPI) is a 13-stage impactor, which operates at 30 L/min, and allows for the collection of PM in 13 size fractions from <0.03 - 10 µm on 25 mm quartz and Teflon filters.

2.3.2 VACES

A Versatile Aerosol Concentration Enrichment System (VACES; figure 3) was used to collect particulate matter (PM) in two size fractions: coarse (2.5 – 10 µm) and fine (<2.5 µm, including ultrafine) particles. The VACES is designed to concentrate PM and to capture the particles in water droplets that can easy be collected in a BioSampler. By collecting the particles in distilled water (or another liquid), agglomeration is reduced, and the particle suspension can directly be used for toxicity studies without the need of further extraction steps which might affect the physicochemical characteristics. The procedure to use VACES to sample PM has been described extensively by Kim et al. (2001). In short, a single nozzle virtual impactor was used to collect the coarse fraction, whereas the fine fraction was collected by drawing air samples through two parallel lines. The fine size fractions go through a saturation-condensation system, which grows particles to 2–3 µm droplets, and which are then concentrated by virtual impaction (Liu et al., 2019). The concentrated output flow from the virtual impactors is connected to a liquid impinger (BioSampler, SKC West Inc., Fullerton, CA) in order to yield concentrated PM suspensions. The coarse particles do not require to be drawn through a saturation-condensation system as they are able to penetrate directly into water. Before each use, distilled water was used to fill the impinger for the coarse mode. To increase the yield of collected PM, two VACES systems were operated in parallel, with per system a sampling flow of ~600 L/min. PM suspensions were stored at -20°C until further analysis.

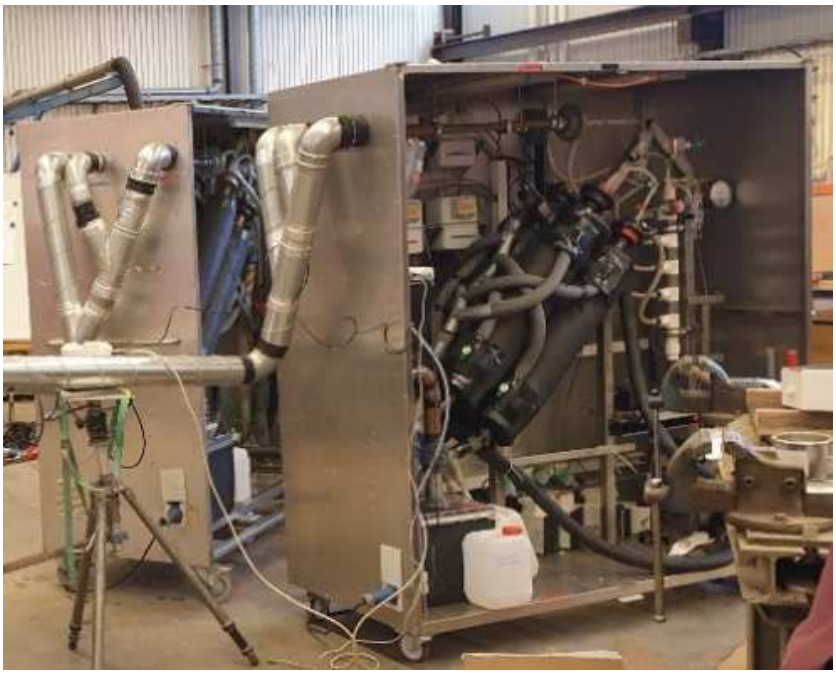

Figure 3. Versatile Aerosol Concentration Enrichment System (VACES)

2.4 Accelerated UV-ageing of PM

To simulate photochemical transformation of PM in ambient air, off-line aging is carried out in an accelerated UV aging chamber. This controlled environment allows for photochemical aging under standardized conditions with full control over temperature and UV light. This will address the specific health hazards at given exposed site by adding the impact from fresh (i.e. local) and aged (i.e. mid/large-range transport) emissions. UV aging was performed on collected TSP on 47mm quartz filters that were placed in glass dishes. Accelerated UV ageing was executed in a UVA Cube (Dr. Hoenle AG, Gilching, Germany) using a Fe lamp (Figure 4). The intensity of the lamp was measured by a UV Power Puck (EIT, Sterling VA). The distance of the samples and the lamp was 15 cm. The Fe lamp has a different spectrum than the sun, as can be seen in figure 5. The intensity of the Fe lamp as measured by the UV Power Puck is shown in Table 3. In Table 4, the cumulative power is shown for the Fe lamp and the sun, including the ratio between the whole light sources.

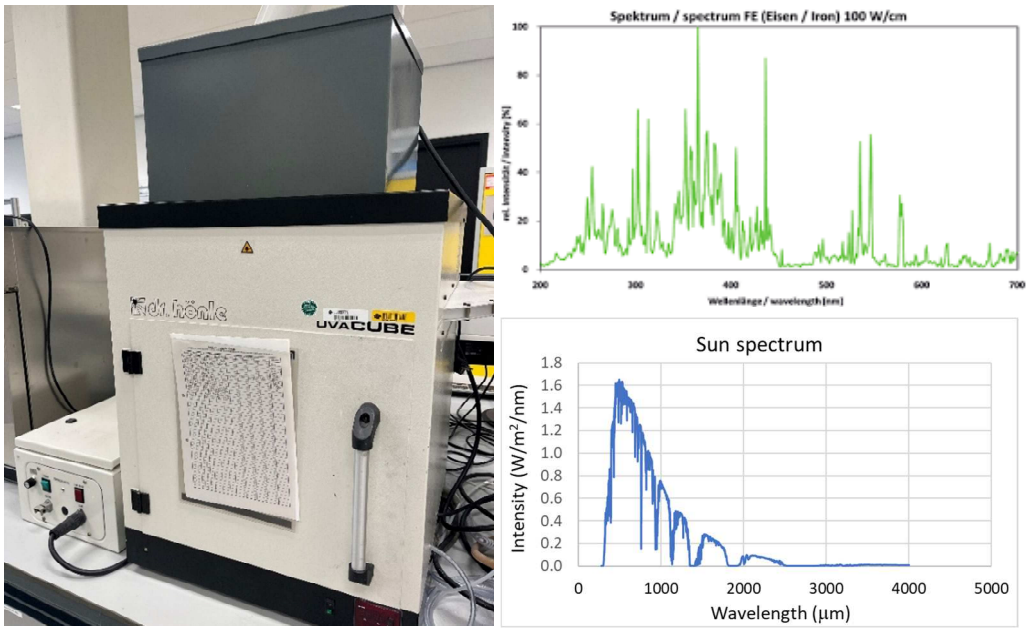

Figure 4. The UVA Cube (left), spectrum of the Fe lamp (top right) and sun (ASTM G173-3, global tilt 37°) (bottom right)

Table 3. Overview of Fe lamp characteristics

Type	Wavelength Range	Energy input (J/cm²)	Average power (W/cm²)	Peak power (W/cm²)
UV-c	250-280 nm	0.096	0.003	0.0032
UV-b	280-320 nm	0.52	0.017	0.021
UV-a	320-390 nm	2.345	0.078	0.095
UV-Vis	390-450 nm	2.184	0.073	0.081

Table 4. Comparison between Fe lamp intensity and the sun

Type	Wavelength Range	Fe lamp (W/m²)	Sun (W/m²)	Ratio
UV-c	250-280 nm	32	5.10^{-23}	∞
UV-b	280-320 nm	170	1.70	102
UV-a	320-390 nm	780	37.2	21
UV-Vis	390-450 nm	730	70	10

The overall ratio of the Fe lamp and the sun in the range between 250 and 450 nm is 15. Thus, the UV degradation of materials in the UVA Cube proceeds 15 times faster than outdoors. The UV exposure is executed in 1 hour time slots over a period of 5 days, having a total exposure duration of 8 hours. The reason for the short exposure times, is the heating of the samples by the UV light. The samples reached a temperature of 85 °C after 1 hour of exposure. This high temperature will also accelerate the thermal degradation of the samples. Typically, every 10 °C increase in temperature will accelerate the degradation by a factor of 2. So, compared to a temperature of 25 °C, an exposure temperature of 85 °C will accelerate the degradation by a factor of 64. Assuming a linear increase in temperature during the 1 hour exposure, an average acceleration factor of 16 was calculated. If a typical summer day of 12 hours of sun at a temperature of 25 °C is assumed, the corresponding number of outdoor days was 10 days of UV ageing and 5 days thermal aging (Table 5). Thermal degradation is generally proceeding much slower than UV degradation, therefore the accelerated ageing of TWP on the quartz filters can be compared to 10 days of outdoor weathering.

Table 5. Exposure characteristics of the aging in the UVA Cube and corresponding outdoor days

Type	Acceleration factor	Exposure time	Outdoor conditions	Corresponding outdoor days
UV ageing	15	8 hours	120 hours	10
Thermal ageing	16	8 hours	128 hours	5

3 Analytical techniques

For the physicochemical analysis of the tires and PM & gaseous emissions from the circular road simulator tests, the analytical and microscopical techniques in Table 6 have been used. In sections 3.1 – 3.8 the different techniques are described in detail.

Table 6. Workflow of the physicochemical analysis performed on tires and PM & gaseous emission from the in-lab testing with the VTI road simulator

	Technique	Chemical compound / characteristics	Relevancy / remark	Tires	PM & gas
	Gravimetrical analysis	Particulate matter (PM)	PM mass concentration		x
	Thermal-optical EC-OC analyser (elemental/organic carbon)	Carbon black (additive) and total rubber content	OC is a measure for rubber + organic additives	x	x
	Ashing and Energy dispersive X-ray analysis (EDX)	Elemental composition and inorganic additives: silica, clay, sulphur (cross linking agent)	Chemical characterisation of tires	x	
	Thermal extraction and desorption GCMS (TGA-TED-GCMS)	SBR/BR, NR and TWP (based on markers 4-PCH and DP)	Concentration of SBR/BR, NR and total TWP in PM	x	x
		SBR/BR, NR, total rubber and additives (based on TGA profile)	Thermographic characterisation of tires & PM	x	x
		Volatile and semi-volatile organic compounds	Non-target screening of (S)VOCs and insight in chemical transformation		x
	Liquid chromatography in combination with tandem mass spectrometry (LCMSMS)	Benzothiazoles & derivatives (vulcanization accelerator)	Benzothiazoles can be used as a tracer (may be released as volatiles when tire gets hot)	x	x
		Amines (anti-oxidants)	Organic pollutants	x	
	Gas chromatography in combination with mass spectrometry (GCMS)	Polycyclic aromatic hydrocarbons (PAH) (extender oils), phthalates (plasticizer)	Organic pollutants	x	
	Thermal desorption gas chromatography in combination with mass spectrometry (DTD/TD-GCMS)	Volatile and semi-volatile organic compounds (oils, resins and additives)	Non-target screening of (S)VOCs and insight in chemical transformation	x	x
	Inductively coupled plasma mass spectrometer (ICP-MS)	Zinc oxide (accelerator activator) and other elements	Zinc (and cobalt) as TWP markers	x	
Microscopic techniques	High resolution scanning electron microscopy with energy dispersive X-ray analysis (FEG-SEM-EDX) combined with automated image analysis	Particle counting and physicochemical properties (PSD, elemental composition)	Characterisation tire related submicron particles and UFP, differentiation TWP and RWP		x
	Infrared microscopy (µFTIR)	Functional groups in molecules	Insight in chemical transformation (oxidation)		x

3.1 Gravimetrical analysis

The concentration of collected PM on Teflon filters is determined using gravimetric analysis in accordance with NEN-EN 12341 (NEN, 2014). The Teflon filters were weighed before and after sampling using a microbalance (Mettler Toledo AX205; ± 1 µg) to constant weight in a conditioned room (50% relative humidity, 20 °C).

3.2 ECOC analysis

Elemental carbon and organic carbon (EC/OC) is determined using thermal-optical carbon analysis according to NEN-EN 16909 (Outdoor air - Measurement of elemental carbon and organic carbon deposited on filters). The temperature program used the EUSAAR 2 protocol. Organic carbon is burned in a temperature range up to 650°C in 4 steps (200°C, 300°C, 450°C and 650°C) in a non-oxidizing carrier gas (helium). Elemental carbon is burned (oxidized) by administering a mixture of helium and oxygen at a temperature range up to 850°C in 4 steps (400°C, 550°C, 700°C and 850°C). For the separation of organic and elemental carbon is done by an optical inspection of the resulting graph.

3.3 TGA-TED-GCMSMS

To determine the mass concentration of TWP, TED-GCMS analysis was performed following the procedure of [34]. The analysis is a two-step method. A sample is first decomposed in a thermogravimetric analyser (TGA) and the gaseous decomposition products are then trapped on a solid-phase adsorber. Subsequently, the solid-phase adsorber is analysed with thermal desorption gas chromatography tandem mass spectrometry (TD-GC-MSMS). A representation of the used TGA-TDU-GCMSMS set-up is shown in Figure .

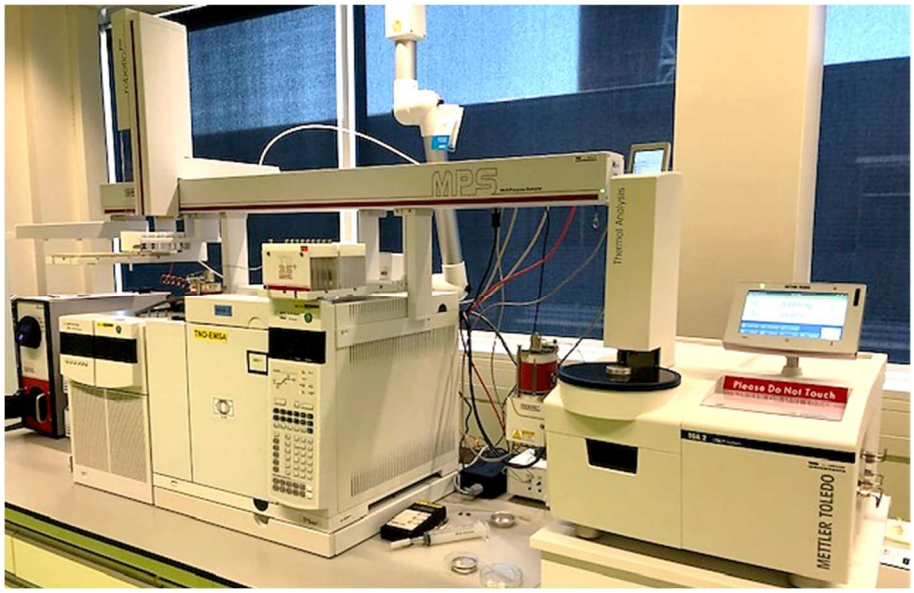

Figure 5. the TGA-TDU-GCMSMS system used for the analysis of rubber and TWP

The measurements were carried out with a thermogravimetric furnace TGA 2 with an auto sampler (Mettler Toledo GmbH, Germany) using 150 or 900µL crucibles and a purge gas flow (N2) of 30 ml min-1. The following temperature program was used: 35°C (2min), 35-290°C (20°C/min), 290°C (2min), 290-550°C (20°C/min), 550°C (2min), 550-1000°C (50°C/min), 1000°C (5min). Between 35-290°C the released gaseous products were discarded and only between 290-550°C the decomposition products were sampled. Between 550-1000°C the purge gas was synthetic air (50ml/min) to burn residual carbon (mainly elemental carbon) in the crucibles and to clean the TGA system. With the same instrument also non-target screening of VOCs and SVOCs have been performed on the freshly generated and aged TSP filters. For that purpose, between 35-290°C the released gaseous products were not discarded but also sampled.

The TGA is coupled to a thermal desorption unit (TDU 3.5, Gerstel, Germany) via a heated transfer line (250°C), a heated coupling (130°C) and a TAU interface that is cooled to 25°C. Tenax TA 100mg (Industry standard; length 3.5inch 1/4inch diameter) was used as solid-phase adsorbent agent. A 7000 GC/MS Triple Quad (Agilent Technologies, United States) was used to analyse the decomposition products. The GC was equipped with a cooled injection system (CIS 4, Gerstel) and a TDU 2 unit (Gerstel). The sample robot for the transfer of the thermal desorption tubes from the TGA to the TDU was designed with a MultiPurpose Sampler (MPS, Gerstel). The thermal desorption was carried out in solvent vent mode with a total He flow of 25 ml min-1. The sample was thermally desorbed with a temperature

program of 50 to 280 °C at a heating rate of 60 °C min-1 and hold time at 280 °C for 10 minutes. The compounds were trapped on a Tenax TA trap in the CIS at -25°C, using a CCD2 system (Gerstel). For the chromatographic separation, a HP-5MS column (30 m, 0.25 mm i.d., df = 0.25 µm) with a flow rate of 1 ml min-1 He was used. The temperature program for the GC was: 40°C (2 min), 40-300 °C (10°C/min), 300°C (2 min). A temperature of 300 °C for the MS source was selected. The MS was used in MRM mode. Dipentene (DP) and 4-phenylcyclohexene (4PCH), also referred as cyclohexenylbenzene) were used as markers for qualification and quantification of natural rubber (NR) and styrene-butadiene rubber (SBR). Identification and quantification of these markers was achieved via a comparison of retention times and MRM transitions with those of an external standard mixture. The following MRM transitions were used: quantifier (m/z) 93-77 (CE 15eV) and qualifier (m/z) 67-41 (CE 15eV) for dipentene; quantifier (m/z) 104-78 (CE 15eV) and qualifier (m/z) 104 – 51 (CE 50eV) for 4PCH.

Different quantification methods can be used to determine the mass of TWP in a sample based on the pyrolysis products measured. An in-depth discussion of these methods is presented in LEON-T Deliverable 3.1 [35]. In this study, two external standard calibration methods were used for the quantification of TWP in collected PM. The first method is based on directly spiked pyrolysis markers (4PCH, DP) in methanol to Tenax TA tubes. The conversion factor (mg marker per gram tire) to calculate the mass of TWP in collected PM is based on the analysis of the actual tires that were tested in the circular road simulator. Each tire has been analysed with TGA-TED-GCMSMS to quantify the amount of different pyrolysis markers 4PCH, DP, styrene, methylstyrene and 4-vinylcyclohexene. The second method is adapted from the Bundesanstalt für Materialforschung und -prüfung (BAM). In this method, the SBR and NR concentrations are calculated using an external standard calibration of reference rubbers SBR1500 and isoprene rubber (IR) in accordance with ISO/TS 21396 and ISO/TS 20593; for SBR a correction factor of 0.9 is applied due to the difference in styrene content between SBR 1500 (23,5%) and SBR in tire tread (15%). The conversion to TWP is based on the actual rubber composition of the different tires, determined with TGA-analysis.

3.4 LC-MS/MS (amines & benzothiazoles)

First, subsamples of tires were cryo-milled to a particle size < 0.25 mm. Around 50 mg of tire particles was weighed and extracted, using a dialysis protocol, with 20 ml of a 1:1 ratio water and acetonitrile. 50 µl of 2-mercaptobenzoxazole (MBO) and benzotriazole-d4 (BZT-d4) (conc. 10 mg/l in ACN) were added as internal standards. The mixture was rotated at 70 RPM for 7 days on a rotating/shaking tray. Without any further sample treatment analysis was performed directly on the 1:1 MQ:ACN extract and on dilution of 200 µl extract with 800 µl 1:1 MQ:MeOH.

Benzothiazoles and amines were analysed with liquid chromatography in combination with tandem mass spectrometry (LCMSMS). Before injection all extracts were filtered through a 0.2-µm PTFE filter. Benzothiazoles were analysed with an Electron Spray Ion source (ESI) in the positive multi-mode source (MMI-ESI-POS) with an Agilent HP1100 Series LC and Agilent 6410 triple Quad LCMS selective detective detector. Amines were analysed in the ESI Jetstream positive mode (AJT-ESI-POS) with an Agilent HP1100 Series LC and Agilent 6410 triple Quad LCMS. Multiple reaction monitoring (MRM) was applied using two ion transitions for each compound. For benzothiazoles and amines a biphenyl reversed phase column (Kinetex 2.6 µm, Biphenyl 100A, 2.1 mm i.d. × 100 mm, Phenomenex, USA) was used and for phenols a Gemini NX-C18 column (3 µm, 100A, 2.1 mm i.d. × 100 mm) was used.

For benzothiazoles separation was performed using a gradient from two different mixtures of water in methanol. One mixture with 5 mM ammonium formiate for 2-aminobenzothiazole (ABT), N-cyclohexyl-1,3-benzothiazol-2-amine (NCBA), 2-(4-morpholinyl) benzothiazole (24MoBT) and 2-(morpholinothio)benzothiazole (OBS) and a second mixture with 100 µl formic acid for 2-hydroxybenzothiazole (OHBT), benzothiazole (BT), 2-mercaptobenzothiazole (MBT), 2-methoxybenzothiazole (MTBT), 2,2-dithiobisbenzothiazole (MBTS), N-cyclohexyl-2-benzothiazolesulfenamide (CBS), 2-benzothiazolesulfonate (2BTS) and again OBS and 24MoBT. Injection volumes were respectively 10 µl and 20 µl. For amines an injection volume of 5 µl and a mixture of milli-Q water (pH 2.5) and methanol both with 0.1% formic acid was used. The following amines were analysed: ethanolamine (ETA), 1,3-diphenylguanidine (DPG), 4-aminodiphenylamine (4-ADPA), 4-hydroxydiphenylamine (4-HDPA), N-(1,3-dimethylbutyl)-N'-phenyl-p-phenylenediamine (6PPD), 2-[(4-Methylpentan-2-yl)amino]-5-(phenylamino)cyclohexa-2,5-diene-1,4-dione (6PPD-Quinone), aniline, cyclohexylamine (CHA), dicyclohexylamine (DCHA), hexa(methoxymethyl)melamine (HMMM), N-Isopropyl-N-phenyl-4-phenylenediamine (IPPD) and triethanolamine (TEA).

The identification of target compounds was accomplished by comparing the retention time and two optimized ion pairs with corresponding standard compounds. Quantification was based on external multiple point calibration lines with required components and associated internal standards. The internal standards were used to monitor the quality of the determination; results for individual samples were corrected based on the recoveries of the internal standards.

3.5 GC-MS/MS (phthalates & PAH)

First, subsamples of tires were cryo-milled to a particle size < 0.25 mm. Around 50 mg of tire particles was weighed and extracted, using a dialysis protocol, with 40 ml of hexane. Prior to extraction, labeled internal standards (all 16 deuterated EPA-PAH, dimethyl ftalaat-d4, diethyl ftalaat-d4, diisobutyl ftalaat-d4, dibutyl ftalaat-d4, butylbenzyl ftalaat-d4, dicyclohexyl ftalaat-d4, bis(2-n-ethylhexyl) ftalaat-d4 and di-n-nonyl ftalaat-d4) were added to the solvent. The mixture was rotated at 70 RPM for 2 x 2 days on a rotating/shaking tray. The two hexane extracts were merged and without any further sample treatment analysis was performed on the resulting hexane extract.

PAH and phthalates were analysed by gas chromatography in combination with mass spectrometry (GCMS) in selected ion mode (SIM) using electron impact ionization (Agilent 6890/5973N) with a semi-polar capillary GC-column (DB-5ms-UI, 30m x 0.25mm i.d. 0.25µm film thickness; Agilent) with 1-2 µL injected in splitless mode using multiple reaction monitoring (MRM) with two ion transitions for each compound. For hopanes/steranes the GC temperature program consisted of an initial temperature of 70°C (1 min) and gradual temperature increase: 25°C/min to 180°C (3min) and 5°C/min to 320°C (5 min). For PAH the GC temperature program consisted of an initial temperature of 60 °C (1 min) and gradual temperature increase: 10 ˚C/min to 100 ˚C and 20 ˚C/min to 320°C (6 min). For phthalates the GC temperature program consisted of an initial temperature of 60 °C (1 min) and gradual temperature increase: 30˚C/min to 160˚C, 5˚C/min to 290˚C, 20˚C/min to 320˚C (3.2 min). For OPE the GC temperature program consisted of an initial temperature of 50 °C (1 min) and gradual temperature increase: 30˚C/min to 160˚C, 5˚C/min to 230˚C (6 min), 10˚C/min to 320 (1.3 min). The identification of target compounds was accomplished by comparing the retention time and two optimized ion pairs with corresponding standard compounds. Quantification was based on external multiple point calibration lines with required components and associated internal standards. The internal standards were used to monitor the quality of the determination; results for individual samples were corrected based on the recoveries of the internal standards.

3.6 (D)TD-GCMS

The sampled Tenax TA adsorption tubes are analysed with an automatic thermal desorption unit (ATD Turbomatrix 400, Perkin-Elmer) coupled with a capillary gas chromatograph (HP 6890, Hewlett-Packard) and a mass spectrometer as detector (Agilent 5973, Agilent technologies). The tube is heated to appr. 340°C under a helium flow for approximately 15 minutes. The desorbed components are captured on a cold trap and injected onto a GC-column (VF624MS, 30-m x 0.25-mm i.d. 1.4µm film thickness; Agilent) via flash heating. The analysis of VOCs is in accordance with NEN-ISO 16000-6 “Indoor air - determination of volatile organic compounds in indoor and test chamber air with active sampling on Tenax TA sorbent, thermal desorption and gas chromatography using MS or MS-FID”. For Direct Thermo Desorption (DTD) of semi-volatiles on quartz filters a part of the filter is placed in an empty thermodesorption tube. The subsequent analysis is the same as the Tenax TA tubes.

Identification and quantification of target components was achieved via a comparison of retention times, qualifier ion ratios and mass spectra with those of an external standard mixture or was based on the TNO-AMDIS library with more than 2500 target compounds + retention indices (RIs). For non-target components identification in screening mode was based on the NIST library with >100.000 compounds. With the instrument settings, identification and quantification of volatile and semi-volatile organic compounds (VOC + SVOC) from 6 - 30 carbon atoms (C6 – C30) is achieved. Organic compounds with all functional groups can be analysed:

- multiple apolair functional groups: alkane, alkene, alkyne, phenyl, alkyl halide
- 1 polair functional group: carboxylic acid, alcohol, ketone, aldehyde, ether, ester, amide, amine, thiol, anhydride, nitrile, pyridine, etc.

For Tenax TA the LOD and LOQ for screening (non-target) mode are ~ 0.1 and 1 µg/m^3. LOQ for target mode is ~ 0.1 µg/m^3 (limited to appr. 20 target compounds each analysis).

3.7 ICP-MS

Subsamples of tires were first ashed in muffle furnace at 580 °C for 6 hours. Subsequently the ash residue is digested with aqua regia (mixture of concentrated hydrochloric acid and nitric acid 3:1) in a Microwave Digestion System. An Element XR High Resolution Inductively Coupled Plasma Mass Spectrometer (HR-ICP-MS; Thermo, Bremen, Germany) was used for the analysis of metals (Li, Be, Zn, Si, Cd, Ba, Pt, Pb, Mo, Na, Mg, Al, P, Ti, V, Cr, Mn, Fe, Co, Ni, Cu, Ag, Sb, B, Sn, W, Zr, S, Au, K, Ca, As, Se, Ce, Pd and Rh). All data acquisitions were carried out in high resolution mode, to avoid the influence of spectral interferences on the results. As an internal standard the element Ge (Germanium) was used. The quantification was carried out by external three-point-calibration. Recovery of heavy metals, was determined with reference material (NIST R1648a).

4 Toxicological Assays

4.1 In-vitro toxicity study

4.1.1 PM concentration

The concentrations of the PM suspensions collected using the VACES were determined from the weight difference of a glass fiber filter after applying 250 µl of PM suspension and drying (at room temperature) until a stable weight was reached. Unfortunately, the PM yield of the sampling campaign was quite low, and the concentrations of PM suspensions were generally too low to enable meaningful in vitro toxicity testing (in the range of 0.02 - 0.15 mg/mL for the coarse fractions, and 0.001 – 0.03 mg/mL for the fine fractions). Therefore, PM suspensions were concentrated using a Christ Alpha 1.2 LD countertop freeze dryer. Samples were freeze-dried until a volume of 1-2 mL was reached. For the coarse fractions, this procedure resulted in PM concentrations in the range of 0.5 – 2.9 mg/mL, which could be used for toxicity testing. For the fine fractions, there was too little material to perform meaningful experiments, even after freeze drying.

4.1.2 Cell culture

A549 cells were purchased from American Tissue Culture Collection (ATCC, Rockville, MD). Cells were cultured in RPMI-1640 cell culture medium supplemented with 10% Fetal Bovine Serum (FBS), 1% penicillin-streptomycin (complete medium) in an incubator at 37°C and 5% CO2/95% air. ALI cultures were obtained by seeding 4.0 x 104 A549 cells (passage 6-15) in 100 µl culture medium on the apical side of 6.5 mm Transwell culture inserts (3 µm pore size, polycarbonate; VWR, Amsterdam, the Netherlands). The basal compartment was filled with 600 µl culture medium. After 36h the medium on both the apical and basal side was removed, cells were washed with Hanks' Balanced Salt Solution (HBSS), and medium was replaced in both compartments. Cells were cultured submerged for 4 days. On day 4, cells were airlifted by removing the apical medium; the basal medium was replaced. Cells were cultured in ALI conditions until exposure on day 6 as described below.

All exposures were conducted in duplicate. The complete experiment was repeated two times, so three independent replicates were performed. Data are expressed as mean ± SEM. Differences between groups were compared by one-way analysis of variance (ANOVA), a p-value < 0.05 was considered statistically significant. Data analysis was conducted using Microsoft Excel

4.1.3 Exposure

Cells were exposed to PM samples by applying different concentrations of PM suspensions in the apical compartment of the transwell inserts (so-called ‘quasi-ALI’ exposure). Only the coarse-sized PM samples could be used for the exposure, as the fine fractions had too little material. Cells were exposed at concentrations of 25, 50 and 100 µg/mL PM in 200 µl (FBS-free) RPMI medium supplemented with 1% penicillin-streptomycin. The basal compartment was filled with 600 µl complete medium. Negative controls were exposed to 200 µl medium only. Positive controls were exposed to 200 µl of 100 µg/mL zinc oxide nanoparticles (NM110, sample ID No. 3055, JRC). Cells were incubated for 24h at 37°C and 5% CO2/95% air. After 24h of quasi-ALI exposure, the apical and basal medium was collected in Eppendorf tubes. After centrifugation for 5 min at 2292g, 70 µl of the supernatant was stored at 4°C and subsequently used for cytotoxicity measurement (LDH assay), and the remainder was stored at -80°C for cytokine analysis (see below). The cells were used for assessment of cell metabolic activity and viability using the WST-1 assay.

4.1.4 Cytotoxicity

Cytotoxicity was measured using the lactate dehydrogenase (LDH) assay (Roche Diagnostics GmbH, Mannheim, Germany), according to the manufacturer’s protocol. Apical and basal culture medium was diluted 1:2 (or 1:10 for positive controls, to prevent a signal above the standard curve) in RPMI medium supplemented with 1% penicillin-streptomycin, and 100 µl of each sample was transferred to a flat bottom 96-well plate (in duplicate). An LDH

standard curve (L-LDH; Roche Diagnostics GmbH) was included on each plate (0.078 – 10 µg/mL LDH, in duplicate). 100 µL of mixed detection kit reagent was added to each well and plates were incubated for 20 min at room temperature in the dark. The reaction was stopped by adding 50 µl of 1M HCl and the plates were read using a microplate reader (SpectraMax 190 Spectrophotometer) at 490 nm. The reference wavelength was set at 600 nm. The absorbance values were corrected for the background signal from wells without cells.

4.1.5 Cell viability and metabolic activity

The cell metabolic activity and viability were assessed using the WST-1 assay (Roche Diagnostics GmbH, Mannheim, Germany), according to the manufacturer's instructions. After 24h of quasi-ALI exposure, 150 µl of WST-1 reagent diluted 1:10 in RPMI medium supplemented with 1% penicillin-streptomycin was added. After a 1 h incubation period at 37°C and 5% CO2/95% air, the volume was transferred to Eppendorf tubes, centrifuged for 5 min at 2292g, and 100 µl of the supernatant was transferred to a flat bottom 96-well plate. The sample's absorbance was measured at 440 nm using a microplate reader (SpectraMax 190 Spectrophotometer). The reference wavelength was set at 620 nm. The absorbance values were corrected for the background signal from wells without cells. The blank consisted of culture medium and an equal amount of the tetrazolium dye.

4.1.6 Cytokine production

The release of a number of cytokines and chemokines was analysed using the LEGENDplexTM Human Essential Immune Response Panel (13-plex) (Cat. no. 740930, Lot B338757, Biolegend, San Diego, California). This allows the simultaneous quantification of 13 cytokines and chemokines essential for immune response, i.e., IL-4, IL-2, CXCL10 (IP-10), IL-1β, TNF-α, CCL2 (MCP-1), IL-17A, IL-6, IL-10, IFN-γ, IL-12p70, CXCL8 (IL-8), and TGF-β1 (Free Active Form). After rehydrating the standard with 250 µL milliQ for 10 min at 300rpm (room temperature), a 1:3 serial dilution was made with assay buffer. Beads were vortexed for 1 min after which a mix was prepared with assay buffer, bead solution and detection antibodies 1:1:1. Of this mixture, 15 µL was pipetted in each well of the 96 well plate (Falcon, V-bottom, pp, REF353263) after which 5 µL of standard, sample or assay buffer as control was added to the wells. This was incubated for 2 h on a plate shaker (Heidolph titramax 100) at 600rpm (room temperature), while the plate was protected from light with the use of aluminum foil for all the coming steps of the assay. Next, 5 µL SA-PE was added to all wells and incubated for 30 min on the plate shaker at 600 rpm (room temperature). Wash buffer was prepared by 20 times dilution in milliQ and 150 µL was added to all wells. The plate was centrifuged for 5 mins at 1000g, setting 7 for acceleration, setting 2 for break (Eppendorf centrifuge 5810R), after which the plate was decanted once to remove the supernatant, pressed onto absorbent paper and turned upside up carefully. Each pellet was resuspended in 80 µL wash buffer and the fluorescence was measured on the FACS Canto II. Data were then processed with the online LEGENDplex software (BioLegend, Qognit), gating was reviewed for inconsistencies in the measurements.

4.2 Oxidative potential analysis

Since the cell-based toxicity tests were limited by the availability of PM material, additional (acellular) investigations of oxidative potential were performed using TSP collected on quartz filters by TNO. OP analysis was conducted on fresh PM samples and after accelerated UV-ageing as described in section 2.4. In addition, OP analysis was also performed on the aqueous PM suspensions which were used for in vitro toxicity testing with A549 cells.

Oxidative potential (OP) reflects the intrinsic ability of PM to generate reactive oxygen species (ROS; e.g. hydroxyl radicals or superoxide) that can cause oxidative stress, which is considered one of the major contributors to cardiorespiratory diseases and a preliminary indicator of potential health effects associated with exposure to PM. Redox-active components and other organic compounds present on the particle surface are the main determinants of OP. A novel immunoassay was used which may be a more reliable and physiologically relevant predictor for toxicity, sensitive to several types of oxidative damage, when compared to some other assays that are often used for OP analysis (e.g. dithiothreitol assay, ascorbic acid depletion assay). In this assay, human serum apoB100 particles – containing low density lipoprotein and very low density lipoprotein – are exposed to PM; oxidized phospholipids are subsequently detected using a monoclonal antibody.

4.2.1 Chemicals

6G6 antibody (anti-apoB100 lipoprotein, Cat# MA5 15851) and monoclonal antibody E06 (Cat# ab02746-21.0) were purchased from Thermo Fisher Scientific (Waltham, MA, USA) and Absolute Antibody (United Kingdom) respectively, and the secondary antibody goat anti-mouse IgM-HRP (Cat# 626820) was obtained from Invitrogen. Phosphate buffered saline and Tween 20 was purchased from Sigma and Thermo Fisher Scientific, respectively.

4.2.2 Extraction and sample preparation

TSP was collected on quartz filters, filters were halved, one half of each filter was subjected to accelerated UV-ageing, and PM amounts on the filters were determined by TNO. Half filters were chopped into four pieces using ceramic scissors and PM samples were extracted in 100% HPLC-grade methanol using ultra bath sonication for 8 min. Extracted samples were stored at 4°C until analysis. Blank filters were subjected to the same extraction procedure. Aqueous PM samples (which were also used for *in vitro* toxicity testing) were collected using VACES and concentrated as described in sections 2.3.3 and 4.1; only the coarse-sized fraction was used (because the yield of the fine PM fraction was too low).

4.2.3 Analysis of oxidative potential (lipid peroxidation measure) using apoB100 particles

The assay was performed as described by Dey et al. [38]. Control human serum (Cat# H5667) samples, free of any disease signature, were purchased from Sigma. In short, high affinity binding microtiter plate wells were coated with 6G6 capture antibody (100 µl of 1:10000 stock) and incubated overnight at 4°C. After washing with PBS containing 0.1% Tween 20 (PBST), the wells were blocked with 100 µl of 1% bovine serum albumin (BSA; fatty acid-free) for 45 min at room temperature (RT). After washing with PBST, 100 µl of diluted serum (1:50) was added and incubated for 1.5 h at RT. Incubation plates were washed 3 times with PBST and incubated with 100 µl of PM sample (25 or 50 µg/ml of methanol- or aqueous extract) for 2h at 37°C with shaking. Fenton reagent ($FeCl_2$:H_2O_2; 1:50) and diesel oil fly ash (DOFA; 12.5 – 100 µg/ml) were used as positive controls. Subsequently, plates were washed thrice using PBST, 100 µl of monoclonal antibody E06 (0.625 µg/ml) was added and incubated for 1.5 h at RT. Then plates were rewashed with PBST and 100 µl of goat anti-mouse IgM-HRP (1:2000 dilution) was added and incubated for 1.5 h at RT. After washing with PBST, 3,3′,5,5′-tetramethylbenzidine (TMB) substrate was added to the plates and after 15 min incubation, 100 µl of stop solution (2N H_2SO_4) was added to the wells. The plates were read at 450 nm using a SpectraMax 190 Spectrophotometer. The data are represented as oxidized phospholipids (Ox-PC, expressed in arbitrary units (AU)), normalized to vehicle (serum without PM sample). The single experiment was performed in triplicates. Data are expressed as mean ± SEM. Statistical analysis was performed by one-way ANOVA with Bonferroni and Tukey's post-hoc test using GraphPad Prism software.

5 Chemical characterisation

5.1 Chemical analysis of tires

The five selected commercial tires and the custom-made tire with 2% cobalt-boroacylate were first extensively chemically analysed using several analytical techniques to determine the complete composition of the tires. Detailed results on rubber content and rubber composition in tires with TGA and TED-GCMS analysis are part of Deliverable 2.2. In Table 7 the general composition of the tires are summarized, based on the TGA analysis

Table 7. Composition of the five commercial tires and the custom-made tire determined by TGA

Description tire	Distribution components in tire (%)				Distribution rubbers (%)	
	SVOC	Rubber	EC	Inorganic	SBR+BR	NR
Temperature (°C)	40 - 330	330 - 750	750 - 1000			
Continental (W)	9%	49%	2.4%	40%	81 ± 3	19 ± 3
Continental (4S)	11%	51%	6.6%	32%	66 ± 11	34 ± 11
Continental(S)	10%	49%	3.1%	39%	76 ± 4	24 ± 4
GoodYear (S)	9%	52%	3.4%	36%	85 ± 4	15 ± 3
LingLong (S)	12%	51%	34%	3%	59 ± 3	41 ± 3
LingLong Cobalt	12%	47%	35%	7%	58 ± 4	42 ± 4

The five commercial tires and the custom-made tire (in duplicate) were analysed for their organic content using GC-MS/MS and LC-MS/MS techniques. The results of the target analysis on selected amines (12 compounds, including 6PPD), benzothiazoles (13 compounds), phthalates (15 compounds) and PAHs (32 compounds, including EPA PAH and REACH PAH) are presented in Table 8 where quantitative results from the two analytical methods have been aggregated. The results for the individual organic compounds and elements are presented in Appendix A. All tires have relatively high amine content ranging from 0.8 – 1.5 % per tire, with the main component 6PDD (~70% of total amines), followed by phthalates and benzothiazoles (~ 0.1% per tire), with the main components benzothiazole and 2-mercaptobenzothiazole (~85% of total benzothiazoles) and diisononyl phthalate and diisodecyl phthalate (~95% of total phthalates). PAHs were only detected in relatively small amounts; only for the custom-made tire PAH concentrations were slightly elevated. Main PAH components are benzo(ghi)perylene, pyrene, fluoranthene, acenapthalene and naphthalene, (~90% of total PAHs).

Table 8. Results of target analysis on amines, benzothiazoles, phthalates and PAHs of the five commercial tires and the custom-made tire determined with GC-MS/MS and LC-MS/MS techniques

Description tire	Amines (mg/g)	Benzothiazoles (mg/g)	Phthalates (mg/g)	PAH TOTAL (µg/g)	PAH REACH (µg/g)	PAH EPA (µg/g)
Continental (W)	13	0,57	1,1	8,2	< 1	8,2
Continental (4S)	13	1,0	1,3	10	< 1	7,2
Continental (S)	14	1,1	0,85	20	< 1	10
Goodyear (S)	15	0,62	0,63	3,3	< 1	3,3
Ling long (S)	12	0,66	1,13	10	< 1	9,2
LingLong Cobalt	7,5 ± 0.8	0,58 ± 0.17	1,6 ± 0.3	76 ± 2	2,2 ± 0.3	57 ± 2

In addition, to target analysis on specific organic compounds, DTD-GCMS analysis has been performed for non-target screening of organic compounds in the five commercial tires. With this analytical technique tire tread material is heated to appr. 340 °C causing SVOCs to evaporate and then be analysed with GCMS. In Table 9 the results of the non-target screening method are presented, where the measured components are classified on the basis of their functional groups. In total 194 organic components were identified, belonging to 17 different chemical classes. Concentrations are expressed as relative percentages, based on GCMS peak areas. The total amount of SVOCs is estimated based on the average concentration : peak area ratio of individual benzothiazoles, amines and phthalates

also analysed with LC-MS/MS and GC-MS/MS. Estimates correspond well with the SVOC content quantified with TGA. As can be seen in Figure 6, main component groups are amines and carboxylic acids (60-70% of total SVOCs). Also high amounts of aromatic compounds, benzothiazoles, alkenes and sulfur compounds (sulfides and thioles) are present (20-30% of total SVOCs).

Table 9. Results of non-target screening of SVOCs in the five commercial tires determined with DTD-GCMS, presented as relative percentages based on peak area

Component group	Components	Continental (W)	Continental (4S)	Continental (S)	GoodYear (S)	LingLong (S)
phthalates	1	0,0%	0,0%	0,1%	0,1%	0,1%
carboxylic acids	15	21%	36%	31%	41%	50%
carboxylic esters	4	0,8%	2,1%	1,6%	0,8%	0,8%
alcohols	20	0,7%	0,3%	0,6%	1,2%	0,3%
aldehydes	11	0,8%	1,6%	1,0%	0,5%	0,3%
ketones	17	0,4%	0,7%	0,6%	1,5%	0,6%
alkanes	17	3,3%	0,2%	0,1%	1,0%	2,0%
alkenes	32	4,4%	5,5%	6,3%	8,7%	20%
aromatics	33	10,6%	10,5%	14%	7,2%	2,5%
ethers	6	0,2%	0,2%	0,1%	0,4%	0,2%
amides	4	2%	0%	1%	0%	0%
amines	8	43%	30%	33%	25%	14%
sulfides & thiols	13	4,5%	8,0%	4,4%	2,4%	1,0%
benzothiazoles	5	4,8%	3,9%	5,3%	8,7%	8,4%
siloxanes	3	0,2%	0,2%	0,2%	0,3%	0,1%
nitriles	5	3,3%	0,5%	0,9%	1,5%	0,0%
total SVOCs (mg/g)	194	90 ± 45	120 ± 60	120 ± 60	80 ± 40	150 ± 75
TGA – SVOCs	-	9%	11%	10%	9%	12%

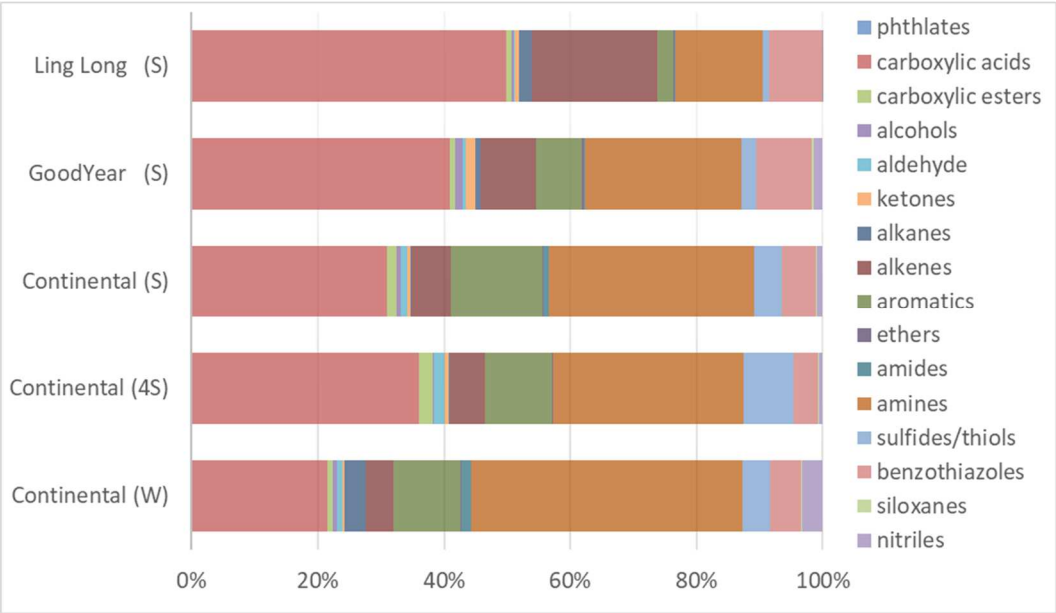

Figure 6. Results of non-target screening of SVOCs in the five commercial tires determined with DTD-GCMS, presented as relative percentages based on peak area

5.2 Characterisation road simulator emissions

5.2.1 Physicochemical characterisation PM

The main results of physicochemical characterisation of collected particulate matter during the road simulator tests with three commercial tires, Continental Winter tire, GoodYear Summer tire and LingLong Summer tire, are summarized in Tables 10 – 12. As mentioned in section 3.3, the quantification of TWP is based on two techniques: the TNO method and the BAM/ISO method. In underlying tables the average concentration of both methods is presented. In addition to TWP, also the concentration of the tire marker benzothiazole has been determined with DTD-GCMSMS analysis to gain more insight into the size distribution of semi-volatile additives of tires. In that respect also the organic fraction of PM has quantified with carbon analysis (elemental carbon and organic carbon).

Table 10. Particle characterisation results of different size fractions of PM, collected during the road simulator test with Continental Winter tires

Continental Winter	Size selective filter samples				Impactor stages < 1µm		
PM fraction	PM1	PM2.5	PM10	TSP	<0.2µm	0.2-0.5µm	0.5-1.0µm
PM - gravimetric (µg/m³)	13.2	21.5	70.8	65.1	10.0	1.9	1.4
EC (µg/m³)	<1.1	1.7	1.5	<1.6	-	-	-
OC (µg/m³)	13.9	17.7	21.5	25.5	-	-	-
TWP average (µg/m³)	0.91	2.3	3.4	4.4	0,32	0,04	0,37
% NR in rubber	5%	4%	9%	6%	9%	11%	7%
Benzothiazole (ng/m³)	2.2	5.0	6.6	7.6	-	-	-

Table 11. Particle characterisation results of different size fractions of PM, collected during the road simulator test with the GoodYear Summer tires

GoodYear Summer	Size selective filter samples				Impactor stages < 1µm		
PM fraction	PM1	PM2.5	PM10	TSP	<0.2µm	0.2-0.5µm	0.5-1.0µm
PM - gravimetric (µg/m³)	17.5	19.3	37.2	39.2	9,0	0,4	0,4
EC (µg/m³)	1.5	1.8	1.9	1.8	-	-	-
OC (µg/m³)	14.1	15.3	16.4	21.8	-	-	-
TWP average (µg/m³)	0.13	0.27	0.43	0.94	0,12	0,02	0,04
% NR in rubber	10%	19%	8%	16%	13%	21%	30%
Benzothiazole (ng/m³)	0.91	0.96	1.1	2.5	-	-	-

Table 12. Particle characterisation results of different size fractions of PM, collected during the road simulator test with LingLong Summer tires

LingLong Summer	Size selective filter samples				Impactor stages < 1µm		
PM fraction	PM1	PM2.5	PM10	TSP	<0.2µm	0.2-0.5µm	0.5-1.0µm
PM - gravimetric (µg/m³)	10.7	16.7	56.6	48.7	9,4	0,2	1,6
PM - AQGuard (µg/m³)	3.7	12.9	48.7		-	-	-
EC (µg/m³)	<0.6	<0.6	0.9	<0.6	-	-	-
OC (µg/m³)	14.3	14.9	15.5	20.4	-	-	-
TWP average (µg/m³)	0.12	0.23	0.62	1.12	0,18	0,01	0,02
% NR in rubber	26%	28%	27%	25%	25%	24%	31%
Benzothiazole (ng/m³)	0.56	0.83	1.1	1.5	-	-	-

The particle size distributions of TWP for the Continental winter tire and the summer tires of LingLong and GoodYear are shown as relative percentages in Figure 7. For comparison the calculated size distributions based on the tire marker benzothiazole are also given. It is clear that the size distributions of benzothiazole is completely different, with a much larger proportion in the smaller size fractions 1 – 2.5 and < 1 µm. Benzothiazole is a semi volatile compound and partly volatilizes during the road simulator tests. A portion of these benzothiazole vapours will condensate and form small aerosols or adsorb on other small particles. This is an example of what happens to other semi-volatile additives in tires. When the tires heat up through abrasion, these additives will gradually volatilize and partially condense again as aerosols. This is supported by the organic carbon analysis. As can be seen in Table 10-12, is that the organic carbon concentration is much higher than the TWP concentration. This can either be the result of the volatilization-condensation process or the result of other emission sources.

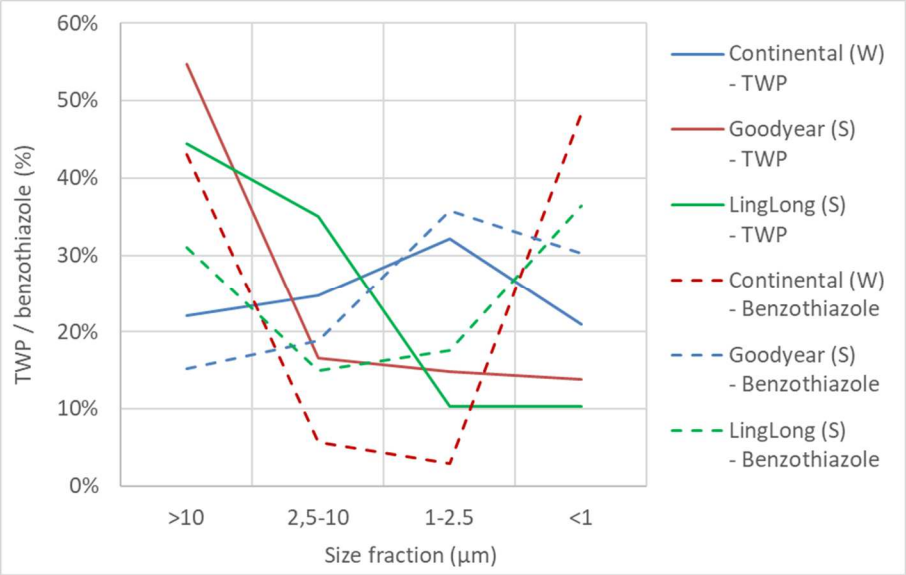

Figure 7. Comparison of the particle size distribution of TWP for Continental Winter (W) tires, GoodYear Summer (S) tires and LingLong Summer (S) tires, determined by TGA-TED-GCMS analysis of rubber (solid lines) and by DTD-GCMS analysis of the tire marker 'benzothiazole' (dotted lines)

5.2.2 Chemical characterisation VOC

In Table 13 and Figure 8 the non-target screening results of the sampled volatiles during the road simulator tests are presented, where the measured components are classified on the basis of their functional groups. In total 218 organic components were identified, belonging to 16 different chemical classes. Results are expressed as relative percentages, based on GCMS peak areas (Figure 10) and also estimated as concentrations (µg/m^3) based on the response of the internal standard toluene. Because not all organic compounds show the same GCMS response as toluene the concentrations should be considered as semi-quantitative. From Figure 16 it can be seen that the composition of the total VOC mixture is similar for all tested tires. Absolute concentrations of volatiles (36 – 81 µg/m^3) are quite high and in the same order of magnitude as PM concentrations (36 – 71 µg/m^3).

Table 13. VOC concentration, classified based on their functional groups, sampled with Tenax TA adsorption tubes during the road simulator tests with the five commercial tires and the custom-made tire, determined with TD-GCMS

VOCs (µg/m³)	Continental (W)	Continental (4S)	Continental (S)	GoodYear (S)	LingLong (S)	LingLong Cobalt
phthalates	0,3	0,3	0,1	0,2	0,3	0,3
carboxylic acids	20,1	9,6	4,7	8,5	7,0	7,7
carboxylic esters	3,5	5,9	1,8	2,7	1,1	2,5
alcohols	6,2	3,0	2,5	4,0	3,9	4,5
aldehydes	8,9	7,9	3,9	4,3	4,5	6,1
ketones	4,1	3,3	2,0	2,9	2,3	5,8
alkanes	6,0	4,4	2,9	5,0	4,0	9,2
alkenes	4,3	3,9	3,3	3,8	3,6	5,2
aromatics	9,7	6,8	5,7	9,3	7,9	11,3
ethers	0,8	0,7	0,4	0,8	0,3	0,4
amides	0,2	0,0	0,0	0,0	0,0	0,0
amine	0,8	1,2	0,9	0,2	0,1	0,9
sulfides/thiols	6,4	2,1	3,4	2,5	2,5	4,2
benzothiazoles	7,8	3,8	2,8	4,1	4,3	7,4
siloxanes	1,4	2,2	1,1	1,3	1,9	3,1
nitriles	0,6	0,0	0,1	0,0	0,0	2,1
total VOCs	81	55	36	49	44	71

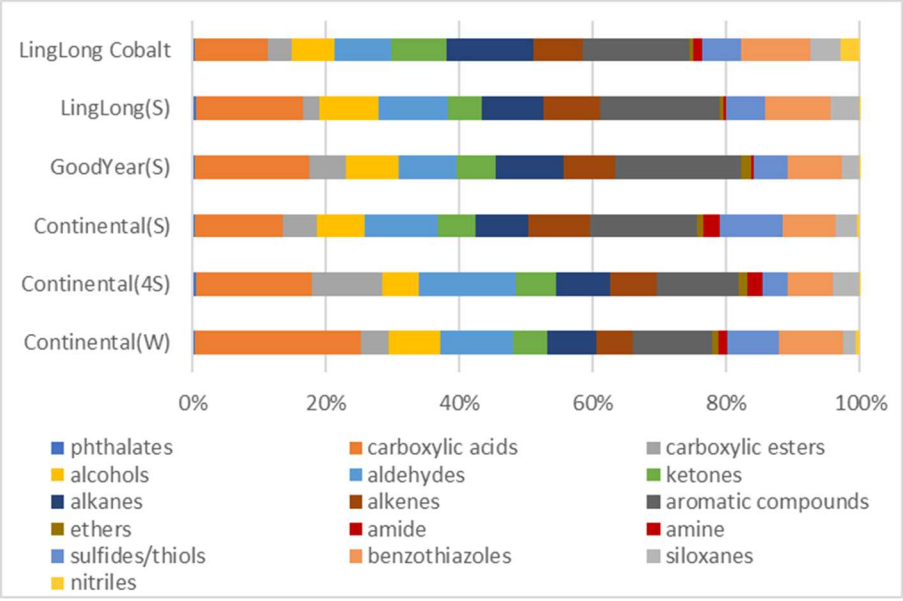

Figure 8. Results of non-target screening of VOCs sampled with Tenax TA adsorption tubes during the road simulator tests with the five commercial tires and the custom-made tire, determined with TD-GCMS, presented as relative percentages based on peak area

5.3 Chemical transformation

The results of the chemical characterisation of the aged and non-aged particulate matter (TSP) are presented in Figure 9 and Table 14 for the three selected tires: Continental Winter (W), GoodYear Summer (S) and LingLong Summer (S). To determine the organic composition TSP filters were analysed with TGA and DTD-GCMS for non-target analysis.

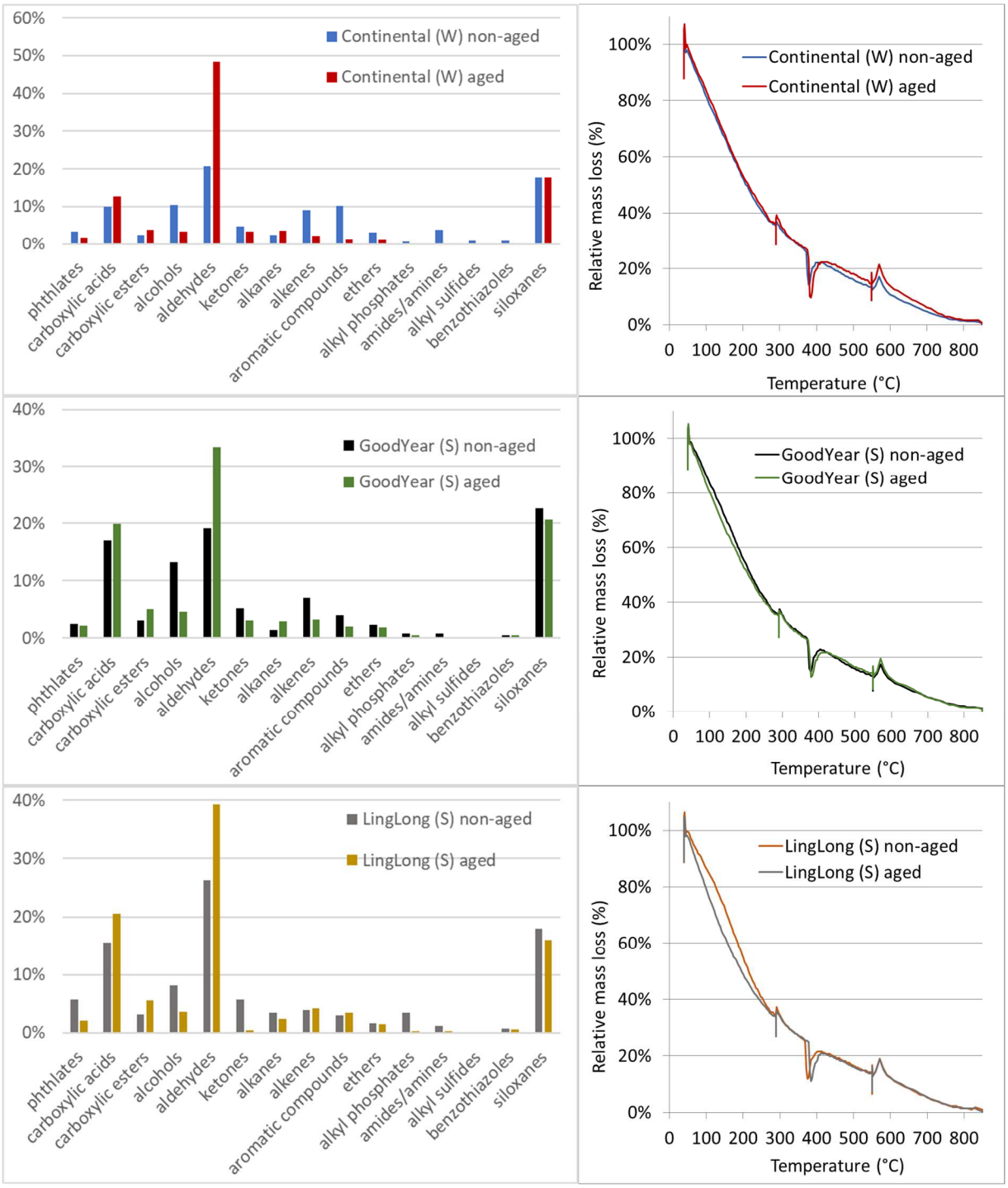

Figure 9. Results of non-target screening of SVOCs determined with DTD-GCMS (left) and TGA analysis (right) of non-aged and UV aged particulate matter (TSP) collected during the road simulator tests with Continental Winter (W), GoodYear Summer (S) and LingLong Summer (S) tires

Table 14. Total SVOCs determined with DTD-GCMS (based on peak area) and results of the TGA analysis of non-aged and UV aged particulate matter (TSP) collected during the road simulator tests with Continental Winter (W), GoodYear Summer (S) and LingLong Summer (S) tires

Temperature (°C)	Component	Continental - Winter		GoodYear - Summer		LingLong – Summer	
		non-aged	aged	non-aged	aged	non-aged	Aged
Thermogravic analysis							
40 - 290	VOC+SVOCs	66%	66%	66%	67%	68%	67%
290 - 650	LVOCs+NVOCs+rubber	27%	25%	26%	25%	24%	24%
650 - 850	EC	7%	9%	7%	8%	8%	9%
DTD-GCMS							
Total peakarea SVOCs		100%	97%	100%	77%	100%	81%

UV aging was performed for 8 hours, which can be compared to approximately 10 days of outdoor weathering. During UV aging the temperature increased to 85°C, which caused some volatilization of the semi-volatile compounds (~3 – 23%). This can be seen in Table 14, where the total peak area of SVOCs of the aged filters, determined with non-target DTD-GCMS screening, are compared with the non-aged filters (set at 100%). The weight loss of the aged and non-aged TSP filters during heating in the TGA show the same pattern (see Figure 11): approximately 66-68% of the total carbon consist of VOCs and SVOCs, that volatilize between 40 -290°C, 24-27% consist of low/non-volatiles (LVOCs + NVOCs) and rubbers, that pyrolyze between 290 – 650 °C and 7-9% consist of elemental carbon. For GoodYear and LingLong summer tires there are some minor changes in the semi-volatile fraction between 40 – 290 °C, which can be caused by changes in chemical composition but also as a result of the volatilization of SVOCs during UV aging. The TGA patterns of the TSP filters are very distinct from the TGA patterns of tire tread (see Deliverable 2.2 for tire tread TGA patterns); for TSP the semi-volatile fraction is much larger than the pyrolysis fraction, for tire tread it's the opposite. This is another indication that SVOCs from other sources than the tires might contribute to the SVOC mass on the TSP filters.

The non-target screening results of the SVOC fraction in aged and non-aged TSP, presented in Figure 11, are classified on the basis of their functional groups. In total 125 organic components were identified, belonging to 16 different chemical classes. Results are expressed as relative percentages, based on GCMS peak areas. For all three tires in the aged TSP filters a big increase in the relative amount of aldehydes is shown and a small increase in carboxylic acids and carboxylic esters. On the other hand, the relative amount of alcohols, alkenes, ketones and aromatic compounds appears to decrease to a greater or lesser extent. In general, this is in agreement with the oxidation pattern during UV aging found in literature, from organic compounds with double bonds, via alcohols, aldehydes/ketones to carboxylic acids. These results indicate that transformation of (semi-volatile) compounds by UV-induced oxidation in the atmosphere can happen and can alter the chemical composition of TWP and other tire-related particles in ambient air. In summary, UV aging causes a higher proportion of oxygenated species.

5.4 Unravelling PM

To be able to identify all the possible sources for the organic carbon fraction of PM, the grease and oil used in the road simulator has been analysed via a non-target screening with DTD-GCMS. In Table 15 and Figure 10 the average results of the non-target screenings of the TSP filters and VOC samples from the five tests with the commercial car tires are compared with the SVOC composition in tire tread, grease and oil. Results are presented as relative percentages of the chemical classes based peak areas, measured with (D)TD-GCMS. The tires and grease/oil cannot explain all the measured VOCs and SVOCs in the TSP filters and VOC samples. For TSP approximately 55% can be explained by the abrasion of tires and the emission of volatiles from oil and grease; for VOCs approximately 85% can be explained by these emission sources. Since the pavement is made from concrete cement without bitumen this source can be ruled out. However, on the floor of the simulator hall remainders of bitumen were present. The road simulator creates air turbulence in the room, which may cause bitumen dust to end up on the PM filters. In general, bitumen consist of aliphatic and aromatic hydrocarbons and can contain oxygenated species like ketones and aldehydes from UV-induced oxidation. This could also be the case for the oil and grease; during the use of the road simulator oxygenated compounds (i.e. carboxylic acid, ketones and aldehydes) are formed by thermal oxidation; this process will also lead to the formation of volatile components [37]. In this case, we analysed the new unused crease

and oil, so the organic composition of the used and aged grease and oil could be different with more oxygenated compounds (e.g. aldehydes). This makes it hard to define the exact source contribution.

Table 15. Results of non-target screening of VOCs sampled on Tenax TA , SVOCs in collected TSP, tire tread material, grease and oil, determined with TD-GCMS, presented as relative percentages based on peak area

Component Groups	Sources			Emission		Source Contribution
	Tire	Grease	Oil	TSP	VOC	
phthalates	0,1%	0,2%	0,0%	3,8%	0,5%	Unknown
carboxylic acids	43,1%	10,5%	1,4%	14,6%	19,8%	Tires + Grease
carboxylic esters	1,2%	5,7%	0,4%	3,0%	4,1%	Grease + Tires
alcohols	0,5%	22,2%	0,3%	10,9%	8,1%	Grease
aldehydes	0,8%	0,0%	0,0%	22,0%	10,0%	Unknown
ketones	0,8%	0,5%	0,1%	5,2%	5,4%	Unknown
alkanes	1,2%	9,9%	13,8%	2,3%	8,9%	Grease + Oil
alkenes	12,5%	20,0%	0,7%	6,6%	7,0%	Grease + Tires
aromatics	6,3%	0,1%	0,0%	4,9%	16,0%	Tires (+ Bitumen)
ethers	0,2%	0,0%	0,0%	2,4%	1,1%	Unknown
alkyl phosphates	0,0%	0,0%	0,0%	1,6%	0.0%	Unknown
amides	0,1%	0,0%	0,0%	0,9%	0,1%	Unknown
amines	21,9%	0.0%	0.0%	0,9%	0,6%	Tires
sulfides/thiols	3,7%	26,0%	83,2%	0,4%	6,4%	Grease + Oil + Tires
benzothiazoles	6,9%	0,0%	0,0%	0,7%	9,2%	Tires
siloxanes	0,2%	4,9%	0,0%	19,9%	2,8%	Grease + Unknown
nitriles	0,5%	0,0%	0,0%	0,0%	0,3%	Tires
Emission	Source distribution (%)			Tire related emission (S)VOCs (µg/m³)		
	Tire	Grease/Oil	Unknown	Continental (W)	GoodYear (S)	LingLong (S)
TSP – SVOCs	20 (15-25)	35 (20-50)	45 (25-65)	4 - 6	3 - 5	3 – 5
VOCs	40 (25-55)	45 (30-60)	15 (0-45)	20 - 45	15 - 30	10 -25

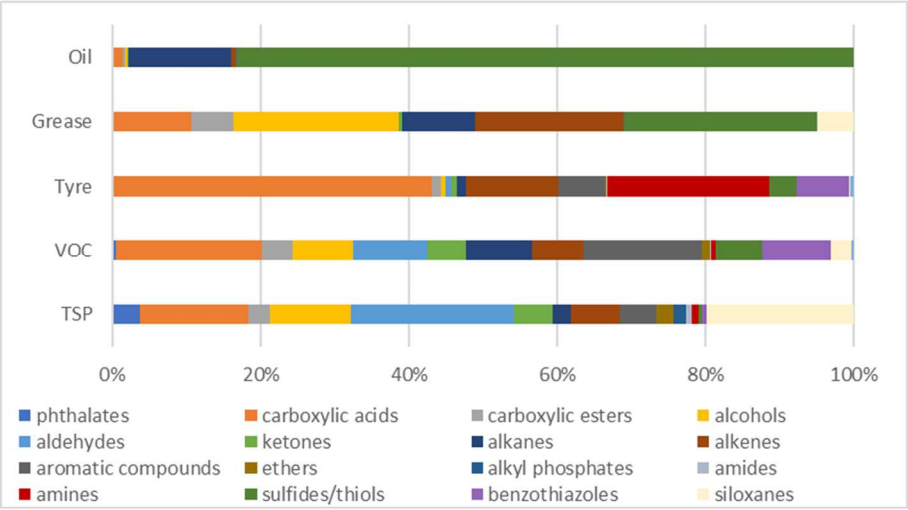

Figure 10. Results of non-target screening of VOCs sampled on Tenax TA , SVOCs in collected TSP, tire tread material, grease and oil, determined with TD-GCMS, presented as relative percentages based on peak area

6 Toxicological examination PM

6.1 In-vitro toxicity

In vitro toxicity tests were conducted using A549 human airway epithelial cells which were exposed to PM collected using two VACES system at VTI's road simulator facility. While PM samples were collected in two size fractions – coarse (2.5 – 10 µm) and fine (<2.5 µm) – only the coarse-sized PM samples could be used for the exposure, since the fine fractions had too little material.

6.1.1 Cytotoxicity

LDH levels, as a marker for cytotoxicity, measured in culture medium of A549 cells exposed to different concentrations of PM were not different from controls. Results obtained in apical medium are shown in Figure 11. The statistically significant ($p < 0.05$) decrease in LDH release after exposure to 100 µg/mL PM from Continental summer tires was considered a chance finding of no toxicological relevance. Exposure to zinc oxide nanoparticles (positive control) resulted in a substantial increase in LDH release ($p < 0.001$). LDH levels in basal medium were slightly lower when compared to apical levels, but showed similar results (data not shown).

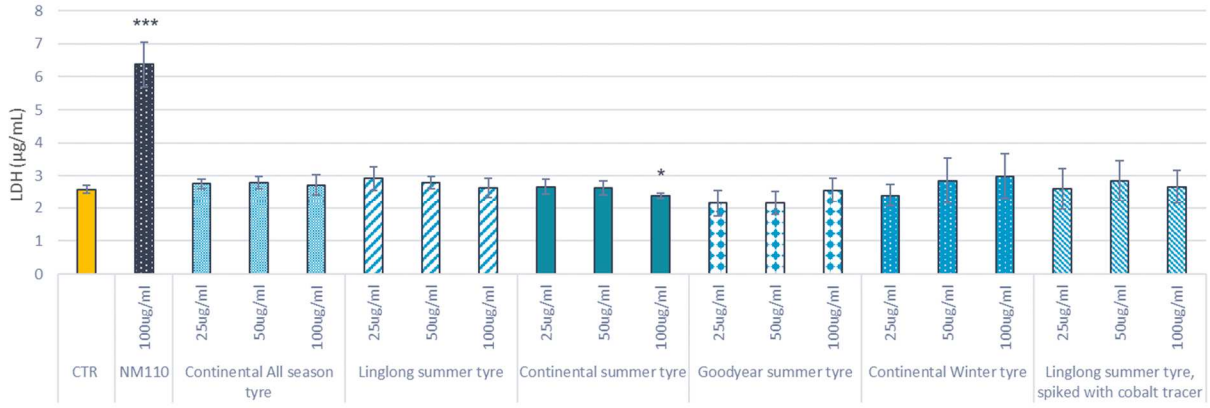

Figure 11. LDH levels in apical medium of A549 cells exposed to different concentrations of PM. Data are expressed as mean ± SEM. CTR: negative control; NM110: zinc oxide nanoparticles (positive control); * $p < 0.05$, *** $p < 0.001$ compared to CTR.

6.1.2 Cell viability and metabolic activity

Metabolic activity and cell viability of A549 cells after exposure to various PM concentrations was evaluated using the WST-1 assay. Though a tendency towards a dose-dependent decrease was observed for some tires, none of the PM samples did have a significant effect on cell metabolic activity (Figure 12). Exposure to zinc oxide nanoparticles resulted in a ~50% decrease in metabolic activity.

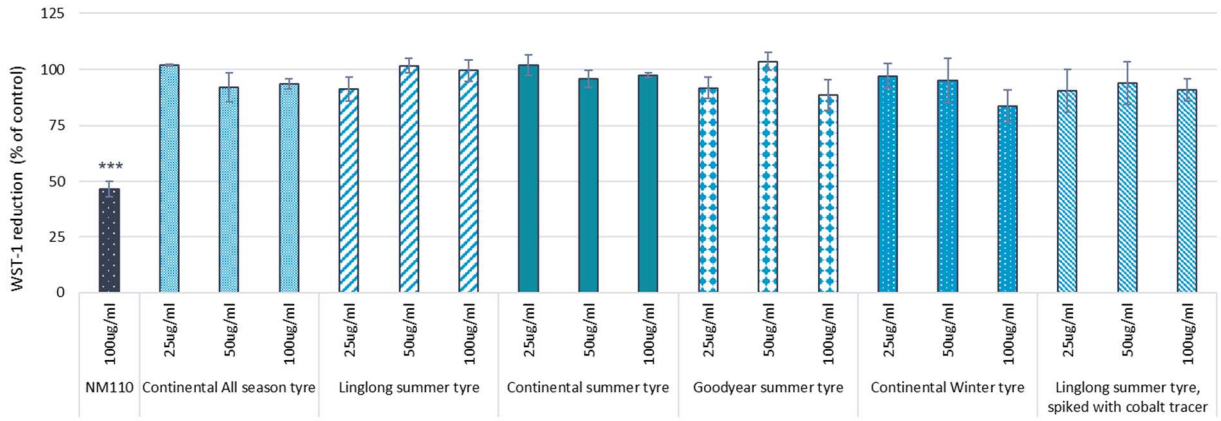

Figure 12. Metabolic activity, assessed by WST-1 reduction, of A549 cells exposed to different concentrations of PM. Data are normalized to the negative control and expressed as mean ± SEM. NM110: zinc oxide nanoparticles (positive control); *** $p < 0.001$ compared to negative controls.

6.1.3 Cytokine production

To characterise the pro-inflammatory response of A549 cells after exposure to PM, the production of a set of 13 different cytokines and chemokines was measured. Of all measured cytokines (IL-4, IL-2, CXCL10 (IP-10), IL-1β, TNF-α, CCL2 (MCP-1), IL-17A, IL-6, IL-10, IFN-γ, IL-12p70, CXCL8 (IL-8), and TGF-β1), only MCP-1, IL-8 and TGF-β1 showed a response 24 hours after exposure. For all three cytokines, concentrations were higher in apical medium when compared to basal medium. Exposure to PM generated from the Continental summer and the Goodyear summer tire resulted in a slight, but dose-dependent and statistically significant increase in the production of IL-8 and MCP-1 (Figure 13). A similar trend was observed for the Linglong summer tire with cobalt tracer, but not for the same tire without tracer, so this finding may be related to the added cobalt. No changes in IL-8 or MCP-1 production were observed after exposure to PM from the winter tires. Production of TGF-b1 was more variable; no statistically significant differences were observed between cells exposed to PM and unexposed controls (data not shown).

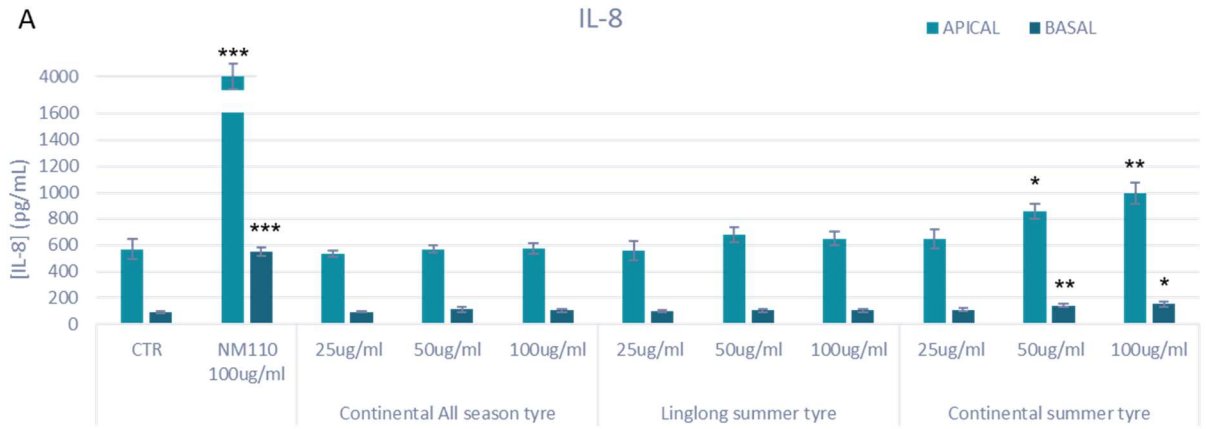

Figure 13. Cytokine concentrations in apical and basal medium of A549 cells exposed to different concentrations of PM. Cytokines were analysed in 96 well plates using a 13-plex LEGENDplexTM kit. Since absolute cytokine concentrations may vary somewhat between plates, negative and positive controls were included on each plate. In the graphs (A-D), TWP samples are compared with controls on the same plate. Data are expressed as mean ± SEM. CTR: negative control; NM110: zinc oxide nanoparticles (positive control); * $p < 0.05$, ** $p < 0.01$, *** $p < 0.001$ compared to CTR.

6.2 Oxidative potential

To assess the oxidative potential of the PM samples, samples were incubated with apoB100 particles and oxidized phospholipids are subsequently detected using a E06 monoclonal antibody. The results are depicted in Figure 14. Incubation with positive control substances induced a marked increase in oxidation of phospholipids (Figure 14A). Exposure to Fenton reagent resulted in a 10-fold increase in Ox-PC when compared to vehicle treatment, and exposure to DOFA induced a concentration-dependent increase in Ox-PC with a substantial effect even at low concentrations, indicating that the assay was quite sensitive in detecting oxidative damage to phospholipids.

Exposure to non-aged TSP resulted in a marginal increase in oxidation of phospholipids for most types of tires; there was no clear concentration-related effect. Interestingly, oxidative potential was significantly enhanced after aging of the TSP samples (Figure 14B). There was no clear difference between the various types of tires. In addition, the coarse-sized PM suspensions which were collected by VACES and were used for *in vitro* toxicity testing (Section 6.1), were also tested in the OP assay. Note that these samples were not subjected to UV-aging. Incubation of apoB100 particles with these PM samples resulted in a 2-4 fold increase in Ox-PC when compared to vehicle controls; there were no clear differences between the various types of tires (Figure 14C).

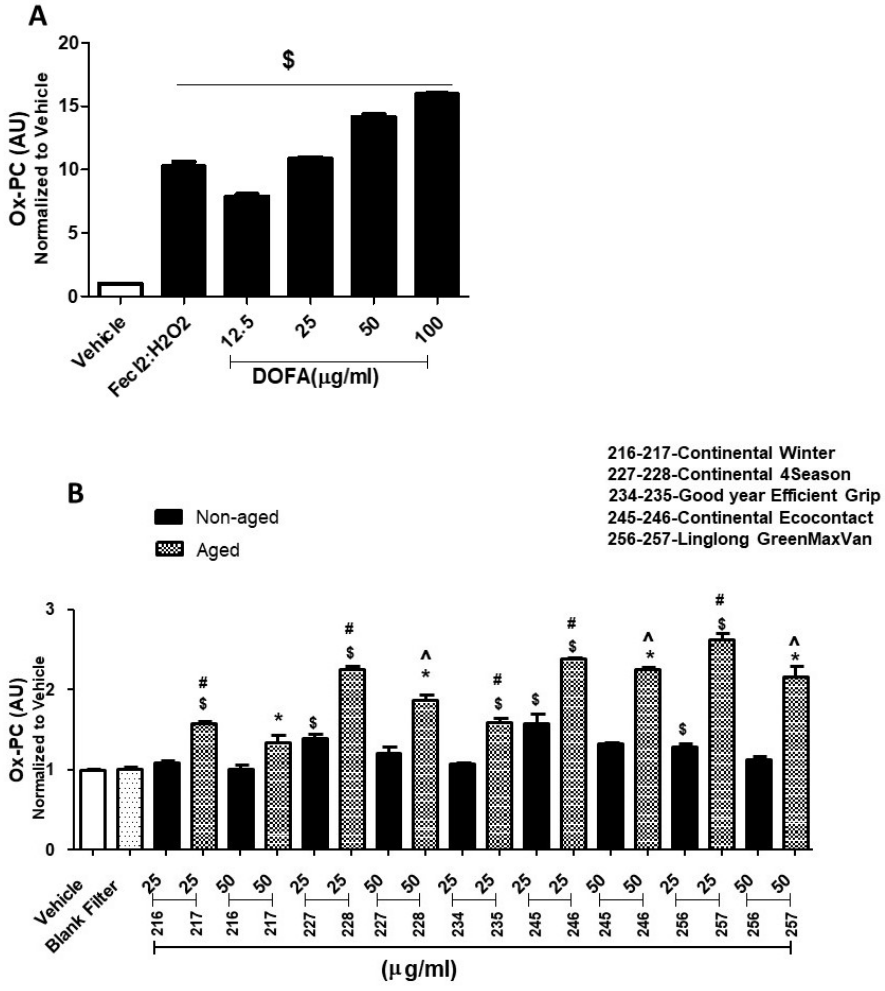

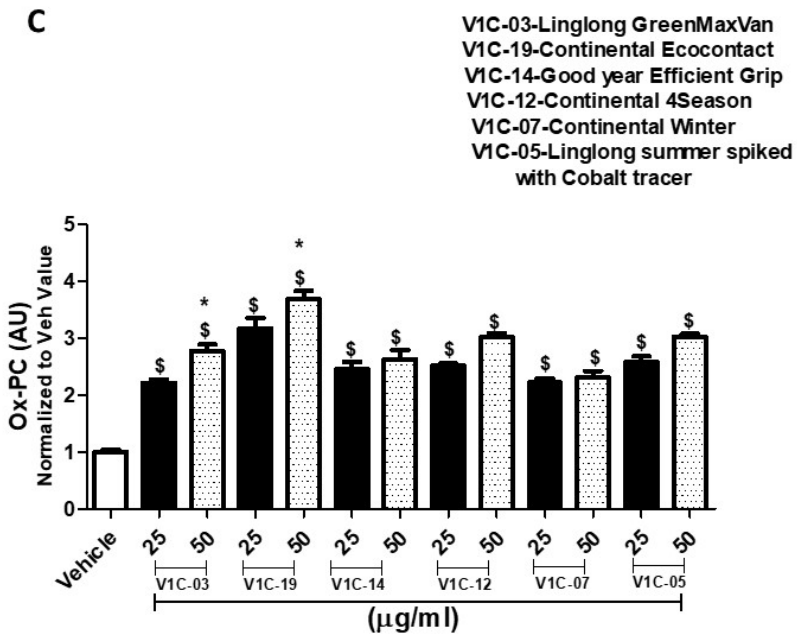

Figure 14: Oxidative potential of PM samples, as determined from oxidized phospholipids on apoB100 particles by an immunoassay as a measure for lipid peroxidation index. A) Oxidized phospholipid (Ox-PC) levels after incubation of apoB100 particles with positive control substances Fenton reagent (FeCl2:H2O2; 1:50) and diesel oil fly ash (DOFA). Data are expressed in arbitrary units, normalized to vehicle. $ $p < 0.0001$ compared to vehicle. B) Ox-PC levels after incubation with 25 or 50 µg/ml of aged or non-aged TSP samples. TSP was collected on filters at VTI's road simulator facility, subjected to accelerated UV-aging, and extracted using methanol. Note that the Goodyear Efficient Grip tire was only tested at 25 µg/ml, because of the limited amount of material available. $ $p < 0.0001$, 25 µg/ml compared to vehicle; # $p < 0.0001$, 25 µg/ml aged vs non-aged; * $p < 0.0001$, 50 µg/ml compared to vehicle; ^ $p < 0.0001$, 50 µg/ml aged vs non-aged. C) Ox-PC levels induced by coarse-sized PM samples (non-aged), collected in aqueous suspensions by VACES. $ $p < 0.0001$ compared to vehicle; * $p < 0.001$, 50 µg/ml compared to 25 µg/ml.

7 Discussion

An in-lab test campaign at VTI's road simulator facilities was organised, to conduct abrasion experiments with different types of tires and from different market segments, to chemically and toxicologically characterise the emitted particles and volatiles and identify potential chemical transformation processes with the objective to evaluate their associated health hazard. Gas and size-selective particle sampling techniques and a VACES-BioSampler was used to collect VOCs and particles on filter and in liquid suspensions which allows for direct in-vitro toxicity testing. The sampled particles on filter were subjected to an accelerated UV-ageing program to simulate the short-term (~2 weeks) UV exposure of particles. Both freshly generated particles and UV-aged TRWP as well as emitted volatiles were analysed on their organic composition using several target and non-target analytical techniques. Toxicity experiments were performed using an *in vitro* model of human lung cells and additional oxidative potential analysis.

Chemical characterisation tires

All tested tires show a similar composition: 47 - 52% rubber, 9 - 12% organic additives and 37 - 42 % filler. For the Continental and GoodYear tires the filler consist mainly of silica with a small percentage (3 - 5%) of carbon black and for the Ling Long tires carbon black is the only component used as a filler. In all tires zinc (vulcanization catalyst) and sulfur (cross-linking agent) are present in almost equal concentrations (1 - 2%). All tires have low concentrations (< 10 ppm) of heavy metals (i.e. Pb, V, Ni, Cr, Cd, Sn); only the lead concentration in the Ling Long tire is a bit higher (81 ppm). The organic additives (used as softeners, stabilizers, preservatives, anti-oxidants, desiccants and plasticizers) have a high content of amines (ca. 3%) and carboxylic (fatty) acids (ca. 3%) with 6PDD, 1,2-dihydro-2,2,4-trimethylquinoline, analine, dibenzylamine, 4-hydroxydiphenylamine, hexadecenoic (palmitic) acid and octadecanoic (stearic) acid as the main identified components. Also the share of aliphatic and aromatic hydrocarbons is large (ca. 2%), with the rubber monomers dipentene, styrene and methylstyrene as main components, followed by benzothiazoles (ca. 0.5%, main components: benzothiazole, 2-mercaptobenzothiazole), organic sulfur compounds (ca. 0.5%, main components: carbondisulfide, octanethiol) and phthalates (ca. 0.1%, main components: diisononyl phthalate and diisodecyl phthalate). In general, there are minor differences in the organic composition of the additives between the winter tire and summer tires. The most pronounced difference are the share of carboxylic acids (two times more acids in summer tires) and amines (70% more amines in winter tires; although differences in chemical compounds can also be the result of differences between brands (Continental, GoodYear, Ling Long).

Chemical characterisation and transformation

In general, total TWP concentrations were low (0.9 – 4.4 µg/m^3) compared to total PM (36 – 71 µg/m^3), with decreasing concentrations in the smaller particulate size fractions (PM10: 0.3 – 3.4 µg/m^3, PM2.5: 0.2 – 2.3 µg/m^3 and PM1: 0.1 – 0.9 µg/m^3). The winter tire produced 5 – 10 times more TWP than the summer and all season tires. For the winter tire also the particle size distribution of TWP was different with the largest share in the size fraction 1 – 2.5µm, while the summer and all season tires produced more coarse material (> 2.5µm). In contrast with the low TWP concentrations, organic carbon concentrations were quite high (20 - 25 µg/m^3), with the majority in the smallest size fraction PM1 (ca. 14 µg/m^3). This can partly be explained by volatilization of semi-volatile additives in the tires during the road simulator tests. A portion of these organic vapours eventually will condensate and form small aerosols or adsorb on other (small) particles. This is in agreement with TGA-analyses, which show that ca. 70 - 75% of the organic carbon consist of SVOCs and 25 - 30% consist of LVOCs (low-volatiles) and NVOCs (non-volatiles), including rubbers.

Absolute concentrations of volatiles (36 – 81 µg/m^3) were quite high and in the same order of magnitude as total PM concentrations. In total 218 volatile organic components were identified, belonging to 16 different chemical classes. Highest concentrations were for carboxylic (fatty) acids and esters (8 – 24 µg/m^3), aliphatic and aromatic hydrocarbons (12 – 26 µg/m^3), carbonyl compounds (6 – 13 µg/m^3), benzothiazoles (3 – 8 µg/m^3), sulfur compounds like sulfides and thiols (2 – 6 µg/m^3) and alcohols (3 – 6 µg/m^3). Slight differences between volatile emissions from the winter tire compared to the summer and all season tires were observed. In general the total emission of VOCs was ca. 80% higher for the winter tire, with ca. two times higher concentrations of carboxylic acids (mainly ethanoic (C2) – nonanoic (C9) acids), sulfur compounds (mainly carbon disulfide) and benzothiazoles (mainly benzothiazole). For the carboxylic acids, this seems in contrast with the difference in chemical composition between the winter tire and summer/all season tires where less carboxylic acids were found in the winter tire. However, these findings were based on the longer chain fatty acids, e.g. palmitic and stearic acid. Although in all tested tires the proportion of the

shorter chain carboxylic acids (C2 – C9) is considerable smaller than the longer chain fatty acids (C10 – C18), in winter tires the concentration of these shorter chain acids is ca. two times higher than in the summer and all season tires. This is in agreement with the observed volatile carboxylic acid emissions.

In aged and non-aged particulate matter in total 125 organic semi-volatile components were identified, belonging to 16 different chemical classes. Highest concentrations in non-aged / aged PM were for carboxylic acids (14% / 8% of SVOCs, main components ethanoic acid and hexadecenoic acid), alcohols (11% / 4% of SVOCs, main component 2-ethyl-1-hexanol), aldehydes (22% / 41% of SVOCs, main components hectanal - nonanal), aliphatic and aromatic compounds (14% / 8% of SVOCs, main components 2-ethyl-1-hexene, m-xylene) and siloxanes (20% / 18% of SVOCs, main components D3, D4 and D8). Similar to the chemical composition in the tires, there are only minor differences in the organic composition of SVOCs between the winter tire and summer tires. Also for emitted particulate matter, the most pronounced difference is the share of carboxylic acids (60% more acids in summer tires). For all three tires in the aged particulate matter a big increase in the relative amount of aldehydes is shown and a small increase in carboxylic acids and carboxylic esters. On the other hand, the relative amount of alcohols, aliphatic and aromatic compounds appears to decrease to a greater or lesser extent. In general, this is in agreement with the oxidation pattern during UV aging, from organic compounds with double bonds, via alcohols, carbonyls to carboxylic acids. These results indicate that transformation of (semi-volatile) compounds by UV-induced oxidation in the atmosphere can happen and can alter the chemical composition of TWP and other tire-related particles in ambient air.

The relatively high concentrations of gaseous and particle-bound aldehydes, alcohols and siloxanes are not part of the chemical composition of tires, indicating that other sources in the facility might emit these chemical compounds. A large part can be explained by the use of oil and grease used in the road simulator, however for approximately 15 - 45% of the emitted particle-bound and gaseous chemical compounds the source is not clear. Approximately 15 - 25% and 25 - 55% of the chemical compounds in respectively particulate matter and in the gas-phase can be explained by the tire wear emissions. Nevertheless, from these experiments it can be concluded that besides emitted TWP (0.9 – 4.4 µg/m^3) from abrasion processes, emitted tire-related organic chemicals from volatilization (10 - 45 ug/m^3) and subsequent condensation/adsorption processes (3 – 6 µg/m^3) can contribute to a large extend to the total tire emissions. Even though the tested tires have been broken in, they are quite new, which means that VOC and SVOC emissions will be lower in real-life as car tires age.

Toxicological examination

As mentioned earlier, during the sampling campaign at the road simulator facility, concentrations of emitted particles proved to be substantially lower than expected. Though low emissions are obviously beneficial with respect to potential health risks of tire emissions, this meant that the yield of PM for toxicity testing was lower than expected and that it was not feasible to conduct the toxicity experiments as initially envisaged. It was intended to perform air-liquid interface exposures of human epithelial airway cells co-cultured with macrophages, and to characterise the toxicity using a large set of readout parameters. However, because of the low PM yield, the testing strategy had to be reconsidered and a slightly less sophisticated cell model (mono- rather than co-culture) and mode of exposure (quasi-ALI) was selected to investigate the toxicity using a limited set of readout parameters. The limited availability of test material, which is often an issue in toxicity testing of various emissions, is an important factor to take into account for future campaigns. Direct on-site ALI exposure to emissions may be a promising – albeit technically and logistically challenging – alternative, which also eliminates the need for PM collection and extraction procedures.

Despite the limited availability of test material, the adaptations of the testing strategy meant that meaningful toxicity data could still be generated for the coarse fraction (2.5 – 10 µm) of emitted PM. Fine particles (< 2.5 µm) were also collected, but the yield was too low to enable *in vitro* toxicity testing. PM was collected in aqueous suspensions which were subsequently concentrated by (partial) freeze-drying. A549 cells were exposed (quasi-ALI) to PM suspensions up to a concentration of 100 µg/mL and toxicity was subsequently characterised using cytotoxicity (LDH release), metabolic activity (WST-1 reduction) and the production of cytokines and chemokines as readout parameters. Exposure to the various PM samples did not induce cytotoxicity and had no effect on metabolic activity of A549 cells. Interestingly however, exposure to PM from Continental summer and the Goodyear summer tires resulted in a dose-dependent increase in the production of the pro-inflammatory cytokines IL-8 and MCP-1. No effects on cytokine production were observed after exposure to PM from winter tires. These findings could neither be explained by the chemical composition of PM nor from the composition of the Continental summer and

Goodyear summer tire itself. PM and tire tread from all tested tires show similar chemical compositions with only minor differences. Compared to the other tires PM emitted from the Goodyear summer tire has a slightly larger proportion (ca. 30%) of carboxylic acids, alcohols and siloxanes. Of these chemical classes, the last two are not related to tire emissions. PM from the Continental summer tire was not chemically characterized. The changes after exposure to PM from summer tires were observed in a limited set of parameters, based on a limited number of observations and for only two types of tires. Therefore, it is recommended to confirm these findings using a larger set of tires, which may be tested up to higher dose levels and using additional parameters (e.g. oxidative stress, DNA damage, omics analysis) to characterise the toxicity. Also, more complex cell models (e.g. co-cultures of – possibly primary – epithelial cells and macrophages) and mode of exposure (e.g. air liquid interface exposure) may be applied. Based on the present *in vitro* experiments, which had to be redesigned due to the limited amount of test material available, it is difficult to conclude on the health hazard potential of tire emissions.

The coarse-sized PM samples investigated in the *in vitro* experiments were also analysed with respect to their oxidative potential using a novel acellular immunoassay based on peroxidation of phospholipids on human apoB100 particles The results showed an increased oxidative potential (OP) of PM when compared to vehicle controls – without any obvious differences between the various types of tires – indicating that oxidative stress may play a role in possible tire PM-induced toxicity. This is in agreement with the chemical composition of PM samples, which show no clear differences between the tested tires. In addition, OP analysis was also performed on TSP subjected to accelerated UV-aging, as well as on non-aged TSP collected on filters. Interestingly, while only marginal oxidation of phospholipids was induced by non-aged TSP samples, oxidative potential was significantly enhanced after aging. These findings can be explained by the difference in chemical composition of the non-aged and aged PM samples. The aged PM contains more oxygenated species, mainly aldehydes, but also carboxylic acids and carboxylic esters. These oxygenated species are more OP-active which provoke more oxidative stress responses in the human body. Oxidative stress plays an important initial role in the development of negative health effects (e.g. respiratory and cardiopulmonary diseases) as a result of exposure to particulate matter [39]. However, as already mentioned before, not all PM is tire related; also other sources (e.g. oil and grease) contributed to the PM load. Especially the observed high concentrations of aldehydes are most likely not related to tire emissions.

8 Acknowledgments

The TNO team would like to acknowledge the contributors to this work package, without whom this research would not have existed. The VTI's road simulator facility colleagues whom conducted the road simulator tests of the tires analysed in this research. The RIVM team whom conducted the toxicity testing and concluded the reporting in section 6 & 7 as well as other LEON-T consortium members that provided valuable input in planning, execution and writing phases of this work. TNO also acknowledges the European Union's Horizon 2020 research and innovation program which funded this research under grant agreement No 955387.

9 References

[1] D. W. Dockery *et al.*, "An Association between Air Pollution and Mortality in Six U.S. Cities," *N. Engl. J. Med.*, vol. 329, no. 24, pp. 1753–1759, Dec. 1993, doi: 10.1056/NEJM199312093292401.

[2] D. W. Dockery, J. Schwartz, and J. D. Spengler, "Air pollution and daily mortality: Associations with particulates and acid aerosols," *Environ. Res.*, vol. 59, no. 2, pp. 362–373, Dec. 1992, doi: 10.1016/S0013-9351(05)80042-8.

[3] C. Pelucchi, E. Negri, S. Gallus, P. Boffetta, I. Tramacere, and C. La Vecchia, "Long-term particulate matter exposure and mortality: a review of European epidemiological studies," *BMC Public Health*, vol. 9, no. 1, p. 453, Dec. 2009, doi: 10.1186/1471-2458-9-453.

[4] C. A. Pope *et al.*, "Particulate Air Pollution as a Predictor of Mortality in a Prospective Study of U.S. Adults," *Am. J. Respir. Crit. Care Med.*, vol. 151, no. 3_pt_1, pp. 669–674, Mar. 1995, doi: 10.1164/ajrccm/151.3_Pt_1.669.

[5] H. Puxbaum *et al.*, "A dual site study of PM2.5 and PM10 aerosol chemistry in the larger region of Vienna, Austria," *Atmos. Environ.*, vol. 38, no. 24, pp. 3949–3958, Aug. 2004, doi: 10.1016/j.atmosenv.2003.12.043.

[6] J. Aldabe *et al.*, "Chemical characterisation and source apportionment of PM2.5 and PM10 at rural, urban and traffic sites in Navarra (North of Spain)," *Atmos. Res.*, vol. 102, no. 1–2, pp. 191–205, Oct. 2011, doi: 10.1016/j.atmosres.2011.07.003.

[7] D. Contini *et al.*, "Characterisation and source apportionment of PM10 in an urban background site in Lecce," *Atmos. Res.*, vol. 95, no. 1, pp. 40–54, Jan. 2010, doi: 10.1016/j.atmosres.2009.07.010.

[8] V. Bernardoni, R. Vecchi, G. Valli, A. Piazzalunga, and P. Fermo, "PM10 source apportionment in Milan (Italy) using time-resolved data," *Sci. Total Environ.*, vol. 409, no. 22, pp. 4788–4795, Oct. 2011, doi: 10.1016/j.scitotenv.2011.07.048.

[9] R. M. Harrison *et al.*, "Non-exhaust vehicle emissions of particulate matter and VOC from road traffic: A review," *Atmos. Environ.*, vol. 262, p. 118592, Oct. 2021, doi: 10.1016/j.atmosenv.2021.118592.

[10] M. M. Scerri *et al.*, "Exhaust and non-exhaust contributions from road transport to PM10 at a Southern European traffic site," *Environ. Pollut.*, vol. 316, p. 120569, Jan. 2023, doi: 10.1016/j.envpol.2022.120569.

[11] S. Singh, M. J. Kulshrestha, N. Rani, K. Kumar, C. Sharma, and D. K. Aswal, "An Overview of Vehicular Emission Standards," *MAPAN*, vol. 38, no. 1, pp. 241–263, Mar. 2023, doi: 10.1007/s12647-022-00555-4.

[12] E. Commission, "Commission proposes new Euro 7 standards to reduce pollutant emissions from vehicles and improve air qualityitle," 2022. https://ec.europa.eu/commission/presscorner/detail/en/ip_22_6495 (accessed Aug. 23, 2023).

[13] R. M. Harrison, A. M. Jones, J. Gietl, J. Yin, and D. C. Green, "Estimation of the Contributions of Brake Dust, Tire Wear, and Resuspension to Nonexhaust Traffic Particles Derived from Atmospheric Measurements," *Environ. Sci. Technol.*, vol. 46, no. 12, pp. 6523–6529, Jun. 2012, doi: 10.1021/es300894r.

[14] M. L. Kreider, J. M. Panko, B. L. McAtee, L. I. Sweet, and B. L. Finley, "Physical and chemical characterisation of tire-related particles: Comparison of particles generated using different methodologies," *Sci. Total Environ.*, vol. 408, no. 3, pp. 652–659, Jan. 2010, doi: 10.1016/J.SCITOTENV.2009.10.016.

[15] J. Panko, K. Hitchcock, G. Fuller, and D. Green, "Evaluation of Tire Wear Contribution to PM2.5 in Urban Environments," *Atmosphere (Basel).*, vol. 10, no. 2, p. 99, Feb. 2019, doi: 10.3390/atmos10020099.

[16] J. M. Panko, J. Chu, M. L. Kreider, and K. M. Unice, "Measurement of airborne concentrations of tire and road wear particles in urban and rural areas of France, Japan, and the United States," *Atmos. Environ.*, vol. 72, pp. 192–199, Jun. 2013, doi: 10.1016/J.ATMOSENV.2013.01.040.

[17] J. Rausch, D. Jaramillo-Vogel, S. Perseguers, N. Schnidrig, B. Grobéty, and P. Yajan, "Automated identification and quantification of tire wear particles (TWP) in airborne dust: SEM/EDX single particle analysis coupled to a machine learning classifier," *Sci. Total Environ.*, vol. 803, 2022, doi: 10.1016/j.scitotenv.2021.149832.

[18] B. Baensch-Baltruschat, B. Kocher, F. Stock, and G. Reifferscheid, "Tire and road wear particles (TRWP) - A review of generation, properties, emissions, human health risk, ecotoxicity, and fate in the environment," *Sci. Total Environ.*, vol. 733, p. 137823, Sep. 2020, doi: 10.1016/J.SCITOTENV.2020.137823.

[19] M. J. Foitzik, H. J. Unrau, F. Gauterin, J. Dörnhöfer, and T. Koch, "Investigation of ultra fine particulate matter emission of rubber tires," *Wear*, vol. 394–395, no. September 2017, pp. 87–95, 2018, doi: 10.1016/j.wear.2017.09.023.

[20] M. L. Kreider, J. M. Panko, B. L. McAtee, L. I. Sweet, and B. L. Finley, "Physical and chemical characterisation of tire-related particles: Comparison of particles generated using different methodologies," *Sci. Total*

Environ., vol. 408, no. 3, pp. 652–659, Jan. 2010, doi: 10.1016/j.scitotenv.2009.10.016.

[21] R. Triebskorn *et al.*, "Relevance of nano- and microplastics for freshwater ecosystems: A critical review," *TrAC - Trends Anal. Chem.*, vol. 110, pp. 375–392, 2019, doi: 10.1016/j.trac.2018.11.023.

[22] R. N. Datta and I. F.A.A., "Rubber additives — compounding ingredients," in *Rubber Technologists Handbook*, J. R. White and S. K. De, Eds. Shrewsbury, Shropshire, UK: Rapra Technology Limited, 2001, pp. 167–208.

[23] P. Klöckner, B. Seiwert, P. Eisentraut, U. Braun, T. Reemtsma, and S. Wagner, "Characterisation of tire and road wear particles from road runoff indicates highly dynamic particle properties," *Water Res.*, vol. 185, p. 116262, Oct. 2020, doi: 10.1016/J.WATRES.2020.116262.

[24] R. Dailey, M. Daniel, and A. P. Leber, "Biodegradability of the antioxidant diaryl-p-phenylene diamine using a modified inherent biodegradation method at an environmentally relevant concentration," *Chemosphere*, vol. 93, no. 6, pp. 1023–1028, Oct. 2013, doi: 10.1016/j.chemosphere.2013.05.072.

[25] F. S. Degaffe and A. Turner, "Leaching of zinc from tire wear particles under simulated estuarine conditions," *Chemosphere*, vol. 85, no. 5, pp. 738–743, Oct. 2011, doi: 10.1016/j.chemosphere.2011.06.047.

[26] M. Selbes, O. Yilmaz, A. A. Khan, and T. Karanfil, "Leaching of DOC, DN, and inorganic constituents from scrap tires," *Chemosphere*, vol. 139, pp. 617–623, Nov. 2015, doi: 10.1016/j.chemosphere.2015.01.042.

[27] K. E. Day, K. E. Holtze, J. L. Metcalfe-Smith, C. T. Bishop, and B. J. Dutka, "Toxicity of leachate from automobile tires to aquatic biota," *Chemosphere*, vol. 27, no. 4, pp. 665–675, Aug. 1993, doi: 10.1016/0045-6535(93)90100-J.

[28] M. Simon, N. Hartmann, and J. Vollertsen, "Accelerated Weathering Increases the Release of Toxic Leachates from Microplastic Particles as Demonstrated through Altered Toxicity to the Green Algae Raphidocelis subcapitata," *Toxics*, vol. 9, no. 8, p. 185, Aug. 2021, doi: 10.3390/toxics9080185.

[29] Z. Tian *et al.*, "A ubiquitous tire rubber–derived chemical induces acute mortality in coho salmon," *Science (80-.).*, vol. 371, no. 6525, pp. 185–189, Jan. 2021, doi: 10.1126/science.abd6951.

[30] L. L. Halle, A. Palmqvist, K. Kampmann, A. Jensen, T. Hansen, and F. R. Khan, "Tire wear particle and leachate exposures from a pristine and road-worn tire to Hyalella azteca: Comparison of chemical content and biological effects," *Aquat. Toxicol.*, vol. 232, p. 105769, Mar. 2021, doi: 10.1016/j.aquatox.2021.105769.

[31] K. M. Unice, J. L. Bare, M. L. Kreider, and J. M. Panko, "Experimental methodology for assessing the environmental fate of organic chemicals in polymer matrices using column leaching studies and OECD 308 water/sediment systems: Application to tire and road wear particles," *Sci. Total Environ.*, vol. 533, pp. 476–487, Nov. 2015, doi: 10.1016/J.SCITOTENV.2015.06.053.

[32] J. Thomas, S. K. Moosavian, T. Cutright, C. Pugh, and M. D. Soucek, "Investigation of abiotic degradation of tire cryogrinds," *Polym. Degrad. Stab.*, vol. 195, p. 109814, Jan. 2022, doi: 10.1016/j.polymdegradstab.2021.109814.

[33] C. Johannessen, J. Liggio, X. Zhang, A. Saini, and T. Harner, "Composition and transformation chemistry of tire-wear derived organic chemicals and implications for air pollution," *Atmos. Pollut. Res.*, vol. 13, no. 9, p. 101533, Sep. 2022, doi: 10.1016/j.apr.2022.101533.

[34] E. Duemichen, P. Eisentraut, M. Celina, and U. Braun, "Automated thermal extraction-desorption gas chromatography mass spectrometry: A multifunctional tool for comprehensive characterisation of polymers and their degradation products," *J. Chromatogr. A*, vol. 1592, pp. 133–142, 2019, doi: 10.1016/j.chroma.2019.01.033.

[35] P. Tromp *et al.*, "LEON-T - Low particle Emissions and lOw Noise Tires - Improved sample pre-treatment, thermo-analytical and microscopic methods for determination of TWPs in environmental matrices. Deliverable 3.1," 2022.

[36] Peng, Z., Lee-Taylor, J., Orlando, J. J., Tyndall, G. S., and Jimenez, J. L.: Organic peroxy radical chemistry in oxidation flow reactors and environmental chambers and their atmospheric relevance, Atmos. Chem. Phys., 19, 813–834, https://doi.org/10.5194/acp-19-813-2019, 2019.

[37] Leon A. Smook , Sathwik Chatra K. R., Piet M. Lugt, Evaluating the oxidation properties of lubricants via non-isothermal thermogravimetric analysis: Estimating induction times and oxidation stability, Tribology International 171 (2022) 107569

[38] Sumit K. Dey, Kavya Sugur, Venkataramana G. Venkatareddy, Pradhi Rajeev, Tarun Gupta, Rajesh K. Thimmulappa, Lipid peroxidation index of particulate matter: Novel metric for quantifying intrinsic oxidative potential and predicting toxic responses, Redox Biology, 48 (2021) 102189, doi: 10.1016/j.redox.2021.102189.

[39] L. He & J. Zhang, Particulate matter (PM) oxidative potential: Measurement methods and links to PM physicochemical characteristics and health effects, Environmental Science and Technology, 2023.

Appendix A - Tire analysis results

	GoodYear (S)	Continental (S)	Continental (W)	Continental (4S)	Ling Long (S)	LingLong Cobalt
Amines (µg/g)						
ethanolamine	<1	<1	1.5	5.8	<1	<1
1.3-diphenylguanidine	2700	1300	1700	13	290	9.8 ± 3.8
4-aminodiphenylamine	31	50	53	75	76	55 ± 7
4-hydroxydiphenylamine	1700	930	1200	860	2500	2500 ± 100
6PPD	9100	11400	10400	11200	7900	3500 ± 500
6PPD-Quinone	6.1	6.0	6.2	7.2	13	10 ± 1
aniline	200	59	81	32	73	55 ± 3
cyclohexylamine	1300	78	42	310	1100	1400 ± 200
dicyclohexylamine	3.1	2.6	1.4	1.1	29	<1
hexa(methoxymethyl)melamine	<1	<1	<1	<1	45	<1
N-Isopropyl-N-phenyl-4-phenylenediamine	2.3	3.2	18	12	2.5	1.5 ± 0.1
triethanolamine	<1	<1	<1	<1	<1	<1
sum amines (mg/gr)	15	14	13	13	12	7.5 ± 0.8
Benzothiazoles µg/g)						
2-benzothiazolesulfonate	66	3.7	4.9	4.6	120	35 ± 11
2-(4-morpholinyl) benzothiazole	<1	<1	<1	<1	<1	<1
benzothiazole	160	180	110	180	230	170 ± 60
N-cyclohexyl-2-benzothiazolylsulfamide	1.0	1	1	1	170	8.7 ± 0.4
2-mercaptobenzothiazole	360	930	440	790	43	340 ± 90
mercaptobenzothiazole disulfide [1)]	11	3.1	0.5	1.0	2.8	3.9 ± 1.2
2-methylthiobenzothiazole	0.86	4.1	2.5	4.8	8.5	3.0 ± 1.1
2-(morpholinothio)benzothiazole	<1	<1	<1	<1	<1	<1
2-hydroxybenzothiazole	11	24	8.5	19	56	17 ± 5
2-aminobenzothiazole	0.55	0.51	0.26	0.36	1.1	0.24 ± 0.08
2-(4-morpholinyl) benzothiazole	<1	<1	<1	<1	<1	<1
N-cyclohexyl-1.3-benzothiazol-2-amine	6.5	0.56	0.27	0.77	20	7.0 ± 2.3
2-(morpholinothio)benzothiazole	<1	<1	<1	<1	<1	<1
sum benzothiazoles (mg/gr)	0.62	1.1	0.57	1.0	0.66	0.58 ± 0.17
Phthlates (µg/g)						
dimethyl phthalate	0.42	0.32	0.74	0.36	0.08	0.38 ± 0.08
diethyl phthalate	0.59	0.91	1.1	1.3	1.2	0.87 ± 0.02
diisobutyl phthalate	0.35	0.98	0.95	0.73	0.96	0.51 ± 0.04
dibutyl phthalate	1.1	0.62	0.64	0.75	1.3	1.0 ± 0.03
dihexyl phthalate	<0.3	<0.3	<0.3	<0.3	<0.3	<0.3
butylbenzyl phthalate	5.7	2.9	3.1	3.4	7.4	12 ± 3
dicyclohexyl phthalate	0.19	0.49	0.76	0.24	0.85	0.44 ± 0.04
bis (2-n-ethylhexyl) phthalate	<0.1	<0.1	<0.1	<0.1	<0.1	24 ± 23
difenyl phthalate	<0.1	<0.1	<0.1	<0.1	<0.1	<0.1
diisononyl phthalate (isomeren)	360	460	630	770	670	950 ± 150
diisodecyl phthalate (isomeren)	240	310	420	510	440	620 ± 100
di-n-nonyl phthalate	0.77	<0.1	<0.1	<0.1	3.4	5.3 ± 0.02
bis (2-ethylhexyl) adipate	18	78	7.2	50	6.1	16 ± 0.1
sum phthlates (mg/gr)	0.63	0.85	1.1	1.3	1.1	1.6 ± 0.3
sum additives (%)	1.6%	1.6%	1.5%	1.5%	1.4%	1.0 ± 0.1%

1) Low recovery of 12%, values are not corrected for the recovery

	GoodYear (S)	Continental (S)	Continental (W)	Continental (4S)	Ling Long (S)	LingLong Cobalt
PAH (µg/g)						
napthalene [1)]	0.47	0.41	<0.4	<0.4	1.3	5.1
acenaftylene [1)]	0.59	1.3	0.92	0.57	1.2	10
acenaftene [1)]	<0.6	<0.4	<0.6	<0.7	<0.6	<0.6
fluorene [1)]	<0.4	1.5	3.3	1.5	<0.5	<0.5
pHenantrene [1)]	<0.3	0.88	0.81	0.72	0.82	5.0
anthracene [1)]	<0.3	<0.3	<0.4	<0.5	<0.4	0.49
fluorantene [1)]	0.29	0.82	0.54	0.73	1.1	7.2
pyrene [1)]	1.5	4.3	2.2	3.1	4.8	24
7H-benzo[c]fluorene	<1.8	<1.5	<1.9	<2.3	<1.6	<1.6
benzo(b)naphto(2.1-d)thiophene	<0.4	<0.4	<0.5	<0.6	<0.4	<0.4
benzo(c)phenantrene	<1.5	3.0	<1.8	3.0	<1.4	<1.4
benzo(a)anthracene [1,2)]	<0.4	<0.3	<.0.5	<0.5	<0.3	<0.4
cyclopenta(c.d)pyrene	<2.4	5.2	3.0	3.6	2.2	16
chrysene [1,2)]	<0.3	<0.3	<0.4	<0.4	<0.3	<0.4
6-methylchrysene	<0.8	<0.6	<0.9	<1.1	<0.6	<0.7
5-methylchrysene	<0.5	<0.4	<0.6	<0.7	<0.4	<0.4
benzo(b)fluorantene [1,2)]	<0.3	<0.2	<0.3	<0.4	<0.4	<0.4
benzo(k)fluorantene [1,2)]	<0.4	<0.3	<0.5	<0.5	<0.7	<0.5
benzo(j)fluorantene [1)]	<0.2	<0.2	<0.3	<0.4	<0.5	<0.4
benzo(e)pyrene [1)]	<0.4	<0.3	<0.5	<0.5	<0.4	1.5
benzo(a)pyrene [1,2)]	<0.3	<0.3	<0.4	<0.5	<0.9	0.75
perylene	<0.4	<0.4	<0.5	<0.6	<0.4	<0.4
indeno(123-cd)pyrene [1)]	<0.2	<0.2	<0.3	<0.3	<1.3	<0.6
dibenzo(ac)anthracene	<0.5	<0.5	<0.6	<0.8	<0.4	<0.5
dibenzo(ah)anthracene [1,2)]	<0.5	<0.4	<0.7	<0.9	<1.4	<1.0
benzo(ghi)perylene [1)]	0.49	1.2	0.49	0.61	<1.6	4.5
anthantrene	<0.8	<0.6	<0.8	<1.0	<0.7	<0.8
dibenzo(al)pyrene	<0.9	<0.6	<0.9	<1.1	<0.8	<0.9
dibenzo(ae)pyrene	<0.9	<0.7	<1.0	<1.2	0.9	1.1
coronene	<0.6	1.0	<0.7	<0.8	<0.6	<0.6
dibenzo(ai)pyrene	<1.4	<1.3	<1.7	<2.1	<1.4	<1.7
dibenzo(ah)pyrene	<0.7	<0.7	<0.9	<1.1	<0.7	<0.9
sum REACH PAH (ug/gr)	< 2	< 2	< 2	< 2	< 2	2.2
sum EPA PAH (ug/gr)	3.3	10	8.2	7.2	9.2	57
sum total PAH (ug/gr)	3.3	20	8.2	10	10	76
sum PAH maximum (ug/gr)	22	31	29	33	31	92

1) EPA PAH
2) REACH PAH

Element (µg/g)	GoodYear (S)	Continental (S)	Continental (W)	Continental (4S)	LingLong (S)	LingLong Cobalt
Al	1800	2900 ± 60	1700	270	210	97 ± 4
As	0.1	0.1 ± 0.01	0.1	0.1	1.9	0.6 ± 0.1
B	1.2	2.7 ± 2.4	0.9	1.1	1.6	100 ± 38
Ba	23	26 ± 0.4	17	16	9.1	3.7 ± 1.7
Bi	0.5	2.8 ± 0.3	0.1	0.6	6.3	0.7 ± 0.7
Ca	2000	630 ± 45	1300	1100	880	350 ± 20
Cd	0.1	<0.1	<0.1	0.3	1.4	0.7 ± 0.01
Ce	0.8	2.7 ± 0.1	0.3	0.7	0.3	0.2 ± 0.1
Co	0.4	1.8 ± 1.7	1.4	2.3	0.6	4100 ± 200
Cr	1.5	1.4 ± 0.1	1.7	2.1	4.9	3.6 ± 0.1
Cu	1.0	0.7 ± 0.2	1.4	0.8	5.9	3.7 ± 1.3
Fe	82	120 ± 3	64	74	190	110 ± 15
K	65	970 ± 23	96	450	600	380 ± 2
La	0.6	1.5 ± 0.1	0.2	0.5	0.2	0.1 ± 0.01
Li	8.9	20 ± 0.1	23	12	4.4	0.2 ± 0.01
Mg	140	86 ± 0.3	78	54	240	600 ± 20
Mn	1.2	1.7 ± 0.1	1.4	1.1	4.6	2.0 ± 0.9
Mo	0.2	0.1 ± 0.01	0.2	0.1	0.3	0.1 ± 0.1
Na	5100	5900 ± 700	5800	3900	1000	670 ± 11
Nd	65	2.2 ± 0.2	2.9	0.5	0.4	0.1 ± 0.01
Ni	2.3	2.2 ± 0.1	1.6	0.8	6.1	9.4 ± 0.1
P	14	43 ± 3	33	22	230	170 ± 3
Pb	5.5	1.6 ± 0.1	2.5	4.1	81	34 ± 2
S	3600	4000 ± 130	3000	3200	1400	1500 ± 120
Sb	0.1	0.1 ± 0.01	<0.1	0.1	0.3	0.1 ± 0.01
Se	<0.1	<0.1	<0.1	<0.1	0.2	<0.1
Si	780	840 ± 160	990	760	280	430 ± 330
Sn	5.3	4.7 ± 1.5	1.2	2.3	3.7	0.2 ± 0.2
Sr	3.9	3.5 ± 0.1	1.9	2.4	3.5	2.0 ± 0.1
Ti	18	14 ± 0.1	23	25	12	8 ± 3
V	0.8	2.2 ± 0.1	0.9	1.9	7.9	7.2 ± 1.1
W	<0.1	0.1 ± 0.01	<0.1	0.1	<0.1	0.2 ± 0.2
Zn	20500	10300 ± 800	7200	9300	19700	24200 ± 200
Zr	2.0	2.5 ± 0.1	1.2	2.6	0.5	0.2 ± 0.1